

CHARACTERIZATION AND PROPERTIES INVESTIGATION
OF AUTOMOTIVE STEEL EXHAUST PIPING FAILURE

MUHAMAD FIKRI BIN KHAIRDDIN

MECHANICAL ENGINEERING
UNIVERSITI TEKNOLOGI PETRONAS
JANUARY 2017

Characterization and Properties Investigation of Automotive Steel Exhaust Piping Failure

by

Muhamad Fikri bin Khairuddin

18561

Dissertation submitted in partial fulfillment of

as a Requirement for the

Bachelor of Engineering (Honours)

(Mechanical Engineering)

JANUARY 2017

Universiti Teknologi PETRONAS

Bandar Seri Iskandar

32610 Seri Iskandar

Perak Darul Ridzuan

Malaysia

CERTIFICATION OF APPROVAL

**Characterization and Properties Investigation
of Automotive Steel Exhaust Piping Failure**

by

Muhamad Fikri bin Khairuddin

18561

A project dissertation submitted to the

Mechanical Engineering Programme

Universiti Teknologi PETRONAS

In partial fulfilment of the requirement for the

BACHELOR OF ENGINEERING (Hons)

(MECHANICAL)

Approved by,

(Assoc. Prof. Dr Othman bin Mamat)

UNIVERSITI TEKNOLOGI PETRONAS

BANDAR SERI ISKANDAR, PERAK

January 2017

CERTIFICATION OF ORIGINALITY

This is to certify that research entitled Characterization and Properties Investigation of Automotive Steel Exhaust Piping Failure being submitted, is my original work been carried out as Bachelor's student at the University of Petronas except as specified in the references and acknowledgement. The original work contains no materials formerly published or written by unspecified sources or persons.

MUHAMAD FIKRI BIN KHAIRUDDIN

ABSTRACT

Incident involving failures of steel exhaust elbow pipe connected to a muffler of Proton Persona investigated carrying raw gas has caused serious disruption within the system. This study looks at developing useful approaches and strategies to forecast failure of exhaust piping system for automotive applications. Existing design, manufacturing process and exhaust pipe material as well as operating condition have been reviewed and analyzed using Non-Destructive techniques (NDT) and Destructive techniques (DT). Vickers hardness test conducted using 100kgf load on the failed materials indicated the exhaust pipe fulfill the tensile strength requirement based on industry specification to carry out intended function. Metallographic analysis conducted using optical microscope as well as Scanning Electron Microscope (SEM) at various magnifications indicated multiple evidences of internal corrosion and micro-fractures on steel exhaust pipe surface. Besides, computational Fluid Dynamics (CFD) results showed that the elbow of the exhaust pipe have been exposed to an extreme exhaust gas flow gradient. The high risk elbow area exposed to high velocity, pressure and temperature simulated by Computational Fluid Dynamics (CFD) simulation coherence to the leakage area of the exhaust pipe. Root Cause Analysis (RCA) showed that phenomenon excessive thinning of steel pipe wall caused by erosion-corrosion mechanism exhaust pipe lead to the perforation of an exhaust pipe. Based on the data collected, it is suggested, proper process design of the product may be implemented during installation and fabrication of exhaust piping system, followed by revising and improving gas stream flow inside the exhaust pipe system as well as using corrosion inhibitor in order to avoid occurrence of same failure in future.

ACKNOWLEDGEMENT

It is my pleasure and privilege to express my sincerest appreciation to my Final Year Project Supervisor, Assoc. Prof. Dr Othman bin Mamat, for giving me the opportunity to participate and involve in such a challenging research, exposing myself to real engineering research background and methodologies. A high gratitude credited to him for valuable feedbacks, guidance and open-minded cooperation during the research.

I would like to thank all lectures who directly or indirectly participated in completing this research. I pay my highest respects to my parents and friends for their support and encouragement through with their well-wishes throughout this research.

My greatest thanks and praise goes to God. Surely we belong to Him and to Him we shall return. To Him, I seek help from the best of helpers.

TABLE OF CONTENTS

CERTIFICATION OF APPROVAL	ii
CERTIFICATION OF ORIGINALITY	iii
ABSTRACT.....	iv
ACKNOWLEDGEMENT.....	v
TABLE OF CONTENTS	vi
LIST OF FIGURES	viii
LIST OF TABLES.....	ix
CHAPTER 1: INTRODUCTION.....	1
1.1 Background Study	1
1.2 Problem Statement.....	3
1.3 Objectives	3
1.4 Scope of Study.....	4
CHAPTER 2: LITERATURE REVIEW	5
2.1 Fundamentals of Exhaust System.....	5
2.2 Failure Modes of Exhaust Systems	7
2.3 Exhaust Pipe Manufacturing Process	8
2.4 Material Properties of Exhaust Pipe	9
CHAPTER 3: METHODOLOGY	10
3.1 Project Flow Chart.....	10
3.2 Project Gantt Charts	11
3.3 Key Milestones.....	13
3.4 Working Principle Failure Analysis	14
3.4.1 Non-Destructive Testing (NDT) Analysis	15
3.4.2 Destructive Testing (NDT) Analysis	17

CHAPTER 4: RESULTS AND DISCUSSION	18
4.1 Review of the Background Information	18
4.2 Material Properties of Exhaust Pipe Analysis	21
4.2.1 Composition Examination.....	21
4.2.2 Vickers Hardness Test	21
4.3 Analysis on Failure Area of Exhaust Pipe.....	26
4.3.1 Visual Examination.....	26
4.3.2 Metallographic Analysis	27
4.4 Analysis of Exhaust Pipe Flow Field Simulation.....	31
CHAPTER 5: CONCLUSION.....	37
5.1 Conclusion.....	37
5.2 Recommendations	38
REFERENCES.....	39
APPENDIX A – Tools and Equipment	43
APPENDIX B – Energy Disperse X-Ray (EDX) Results	45
APPENDIX C – Vickers Hardness Conversion	46
APPENDIX D – Properties of Exhaust Pipe Material	47

LIST OF FIGURES

Figure 1.1: Exhaust pipe system [1].....	1
Figure 1.2: 'Bath Tub' curves [7].....	4
Figure 2.1: Exhaust pipe component [8].....	5
Figure 2.2: Manufacturing process (a) Seamless (b) Seam [14].....	8
Figure 3.1: Project flow chart.....	10
Figure 3.2: Key milestones	13
Figure 3.3: Vickers hardness testing mechanism [25]	17
Figure 4.1: Fault tree analysis (FTA).....	19
Figure 4.2: Condition of exhaust pipe studied	20
Figure 4.3: Different size of imprint diameters.....	22
Figure 4.4: Load vs HV values graph	23
Figure 4.5: Log d vs Log P graph	23
Figure 4.6: Diameter vs HV Values graph.....	24
Figure 4.7: Schematic diagram thickness reduction of exhaust pipe	26
Figure 4.8: (a) Surface morphology of exhaust pipe (b) Linking of pits (c) Various size of pits formation.....	28
Figure 4.9: (a) Surface oxidation (b) Decarbunisation.....	29
Figure 4.10: (a) Direction of gas stream flow (b) Erosion-corrosion traces (c) Surface cracks.....	30
Figure 4.11: Exhaust pipe model	32
Figure 4.12: Meshed exhaust pipe model	33
Figure 4.13: Velocity contour	34
Figure 4.14: Turbulence contour.....	34
Figure 4.15: Temperature contour.....	35
Figure 4.16: Pressure contour	36

LIST OF TABLES

Table 2.1: Exhaust Component functionality and service temperature [15].....	9
Table 2.2: Exhaust component's material requirements [16]	9
Table 3.1: Project Gantt chart FYP (1)	11
Table 3.2: Project Gantt chart FYP (2)	12
Table 4.1: Preliminary data of the exhaust pipe.....	20
Table 4.2: Chemical composition of the samples	21
Table 4.3: Vickers test (1) conditions	21
Table 4.4: Vickers test (2) conditions	24
Table 4.5: Vickers hardness values	25
Table 4.6: Requirement of material strength [31].....	25
Table 4.7: Engine specification.....	31
Table 4.8: Exhaust pipe parameters	31
Table 4.9: Mesh result and properties of exhaust model	32
Table 4.10: Operating conditions of gas stream flow	33

CHAPTER 1: INTRODUCTION

1.1 Background Study

An exhaust system is commonly used in a variety of vehicles, construction and agricultural equipment, ships, aircrafts, stationary machinery, and other applications. Figure 1.1 schematically shows an exhaust system in an automotive application. An exhaust system is used to clean and channel exhaust gas out of the vehicle to the atmosphere, diminish noise, and makes the drivers and passengers comfortable, and be able to cope with combustion heat. Vehicle components are physically joined to complete the integrated system by each of them carry out specific functions.

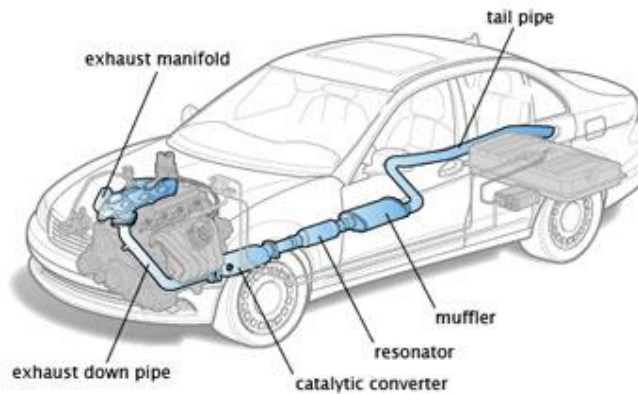


Figure 1.1: Exhaust pipe system [1]

An increasing demand for durability, lightest and cost effective designs of automotive products has led to numerous of powerful techniques used to solve structural durability problems. However, factors such as different types, sizes, operational conditions such as temperature, load and environment, and design details result in a wide spectrum of potential failures, which are frequently difficult to examine and access. Failure can be define as gap between expectation and performance which represents the situation where products such exhaust system components fail to fulfill their functionality during their intended service life. Therefore, improving fundamental

understanding on the system through theoretical modeling, simulation and experimentation enables reuse of the knowledge as strong references and contribution in future researches for further diagnostic review and development process, thus increase overall efficiency of the system.

Failure often has been described in terms of functions and failure of materials and structures. The failure of functions is related to system's malfunction such as power and control, while failure of materials and structures is associated with the loss of capability in load bearing and structural integrity. Failure mechanisms and failure modes are often used interchangeably [2]. However, in this study, in order to differentiate between the appearance of failure and root causes of failure, the two definitions are treated separately. In other words, failure mechanism is described as mechanical, chemical, physical, or other processes that cause failure while failure mode is defined as the pattern, location, or other visible characteristics of the failure [3]. Such define as a system, exhaust system made up chain of components, which are working together. Therefore, performance and safety of exhaust systems and thus the vehicles depend on the reliability of each of the exhaust components which must work together perfectly to achieve the objective of the system.

Failure mechanisms and modes of exhaust pipe determine from the driving factors such materials, loading condition, and operating environment. Record shown that mostly exhaust system failure is mainly due to cracks at welds between pipes and other exhaust components such mufflers. Cracks at hanger-to-pipe and broken hanger rods observed frequently is correlated to fatigue of the system [4]. Generally, exhaust system failure caused by different failure mechanisms, such as corrosion, creep, oxidation, erosion, wear or their combinations. Vibration environment caused by engine vibration, road condition, thermal cycling contribute to cycle-dependent failure mechanism known as fatigue failure. Corrosion, creep, and oxidation are classified time-dependent failure phenomena [3]. Operating at high temperature, vehicle manifolds were frequently faced with failure issues such creep and oxidation of metals [5]. Corrosion in vehicle observed exhaust systems is typically affected by salt, condensate, urea, and other corrosive agents.

In this research, root cause of failure mechanisms and modes of a vehicle exhaust pipe were examined. Theoretical modeling, simulation procedures and experimental investigations were carried out on sub-systems or components instead of a full physical system in order to establish useful concepts and prevention strategies for product design and validation purpose.

1.2 Problem Statement

Automotive industry continuously faces new challenges as the demand for low-cost and good quality metal components increases. Nowadays, the complexity of automobile exhaust systems increased as demands from authorities on emission control, and low vibration and noise levels has become more stringent [6]. In addition, an increasing demand for durability, lighter and cost effective designs of automotive products make determination of root cause of the system failures need to be carry out quickly and precisely, as proper corrective measures need to be developed to avoid future occurrences of failures. Manufacturers reckoned developing designs through testing using prototypes is not effective in accelerating the product development but will increase the non-value added to the product. Therefore, failure analysis is one of the techniques used to construct appropriate solution or prevention steps to eliminate the failures or to minimize the damages if they become investable.

1.3 Objectives

In this research, there are several objectives that need to be achieved. The objectives are as follows:

- To perform failure analysis investigation by Destructive and Non-Destructive Analysis.
- To simulate operating conditions for an exhaust pipe system using Computational Fluid Dynamics (CFD) Analysis.
- To investigate the root cause and source of the failure using Root Cause Analysis (RCA) method.
- To propose an appropriate solutions and prevention strategies for the failure analysed.

1.4 Scope of Study

This research concentrates on characterization and properties investigation on the failure of ferrous metal for automotive application. The research involves the use of Failure Analysis and Root Cause Analysis (RCA). Failure analysis process aimed to understand the nature of the material and thus discover the possible root cause of the failure on the product and suggesting solution and prevention steps through Root Cause Analysis (RCA) to avoid recurrence of the same failures in the future. A careful assessment of the material characteristics following all required standard procedures of failure analysis were applied. Figure 1.2 shows the pattern of failure represented by failure curve known as 'Bath Tub' curve.

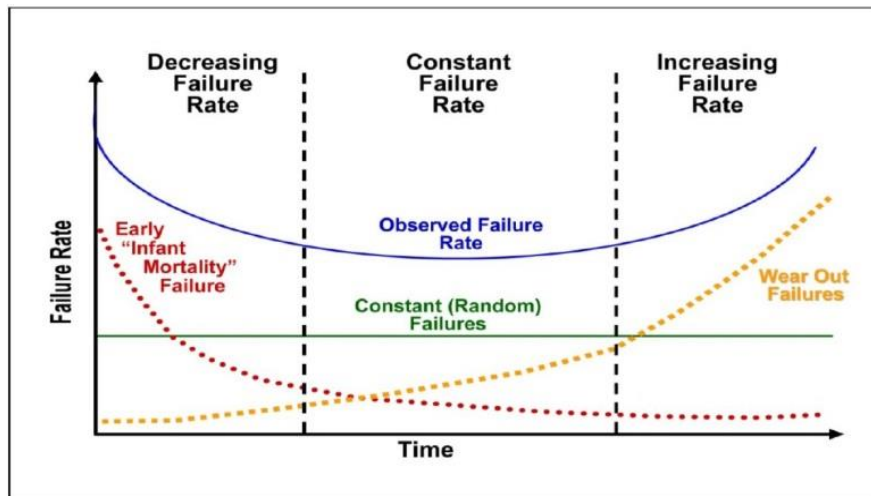


Figure 1.2: 'Bath Tub' curves [7]

The reliability of component can be increased by minimizing the failure in the first zone and extending as much as possible the service life of component represent by second zone. Failure analysis case where professional investigation on the failed components will be carried out is aimed to improve the element of high structure qualities and high safety factor.

CHAPTER 2: LITERATURE REVIEW

2.1 Fundamentals of Exhaust System

An automotive exhaust is generally made of exhaust manifolds, front pipes, catalytic converter, middle pipe, main muffler, and tail pipe as shown in Figure 2.1. Known as hot end region, parts from exhaust manifold to catalytic should have a working temperature above 600 ° C commonly made up from heat-resisting steel. Operating under high frequency and exposed to high temperature of exhaust gas, exhaust manifold is one of critical component in the system that needs to be manufactures by high temperature fatigue resistance materials. The high temperature exhaust gas travel through exhaust manifolds to a muffler along the tailpipe extension with a reduced temperature level before it is emitted to atmosphere.

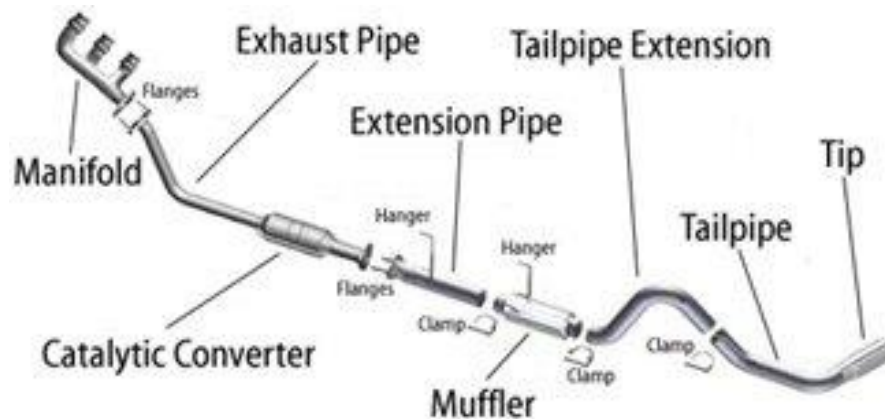


Figure 2.1: Exhaust pipe component [8]

Hot end refers to the region between manifold and catalytic converter. Manifold is regarded as the hottest component at the hot end of exhaust system, possibly reaching temperature of 1000 °C or higher. Not only exposed to high operating

temperature and temperature variations, manifold is simultaneously exposed to external load either caused by applied stress due to the engine and road vibration which creates stress in the components. Low-cycle thermal-fatigue failure observed recently caused by the non-uniform thermal expansion and contraction of exhaust components and systems due to thermal cycles such as engine start-up and shut-down cycles.

From recent studies, there is no doubt that oxidation, fatigue, creep or their combinations can be a major cause of the material failure due to complex thermal-mechanical loading and environmental conditions. However, opposite phenomenon could be observed at the cold end of exhaust system. At the cold end, exhaust is exposed to pitting corrosion, crevice corrosion, and corrosion. Muffler which used for lowering the amount of noise emitted by the exhaust, could be subjected to severe corrosion both externally and internally causing the lifespan of a muffler to be shorter than that of other parts of exhaust systems [9].

The muffler considered as one of critical parts experiencing crevice corrosion which lead to the perforation of mufflers. This issue is also faced by exhaust pipe that connects catalytic converter to muffler. Perforation both in muffler and exhaust pipe not only caused by corrosion but also the variation in temperature, pressure and velocity of the gas due to deficiency in design material and components. Internal corrosion is mainly caused by gas condensate meanwhile while chloride-containing de-icing salts on the roads leads to corrosion observed on exterior surface. Perforations caused by corrosion contribute to noise problems and pressure change in addition with to exhaust gas leakage that can cause concerns as this may allow gas to enter the vehicle.

2.2 Failure Modes of Exhaust Systems

Exposure to high temperature gradients the system component has to withstand one of the root causes to failures of exhaust pipe system when exposed. Common structural failures recorded are cracking and leakage of the components. These failures were likely due to deficiencies in design of the parts and boundary conditions and poor material selection during planning and designing phases. Therefore, there is lacking of comprehensive understanding on the nature of the component to be able order to suggest appropriate solutions for the root cause of failures.

Thermo-Mechanical (TMF) Cracking – The excessive yield stress applied caused the exhaust pipe to degrade due to thermal loading exerted on the system. Crack on the system mainly initiated as few areas to show local cyclic plastic straining of the material caused by cyclic thermal loading. An excessive thermal loading led to fatigue of the exposed material. Therefore, design parameter one of important aspects in order to determining target-oriented strategy by locating the high loaded areas [10].

Leakage – Perforation of exhaust system is frequently related to cyclic plasticization of exhaust manifolds. The leakage problem leads to destruction of the gasket and the flange thus contributes to cracking of manifold due to changed force flow in the system [11]. Therefore, in order to counter the problem, an initial understanding of the problem is needed to determine influencing parameters like welding quality, vibration between parts and nonlinear flow stream vitally considered along the failure analysis process.

High Cycle Fatigue (HCF) – It is defined by low amplitude high frequency elastic strains. High-cycle fatigue involves a large number of cycles ($N > 10^5$ cycles) and an elastically applied stress [12]. High cycle fatigue at the exhaust pipe system is as due to dynamic excitations. Although the problem rarely observed operating system, but deficiency bracket design is one of leading causes to the most of the system.

2.3 Exhaust Pipe Manufacturing Process

Manufacturing of metal pipe can be classified into welded (seamed) and seamless.

Seamless pipe tube

In order to create hollow shell, seamless tube is made by drawing a billet over piercing rod. Seamless tube pipe is formed either by die method or hydroforming method and it does not require welding process. It can withstand high pressure and it is perceived to be robust and reliable [13]. It considered have high thickness and greater diameter, as well as easily available for general use in comparison to seam tubes.

Seamed pipe tube

The seam tubes are manufactured by heating a metal billet at high temperatures [13]. In order to produce hollow tubes, piercing rod or mandrel is used to draw the rotated red-hot billet. Normally, hot rolled or cold rolled metal sheets are used. The shell is moved by hot rolled or cold roller and thus reducing or sizing stands to achieve the preferred wall thickness and diameter. A suitable welding process is selected, according to the material properties of the metal sheet used. Figure 2.2 illustrate the steps involved in tube manufacturing.

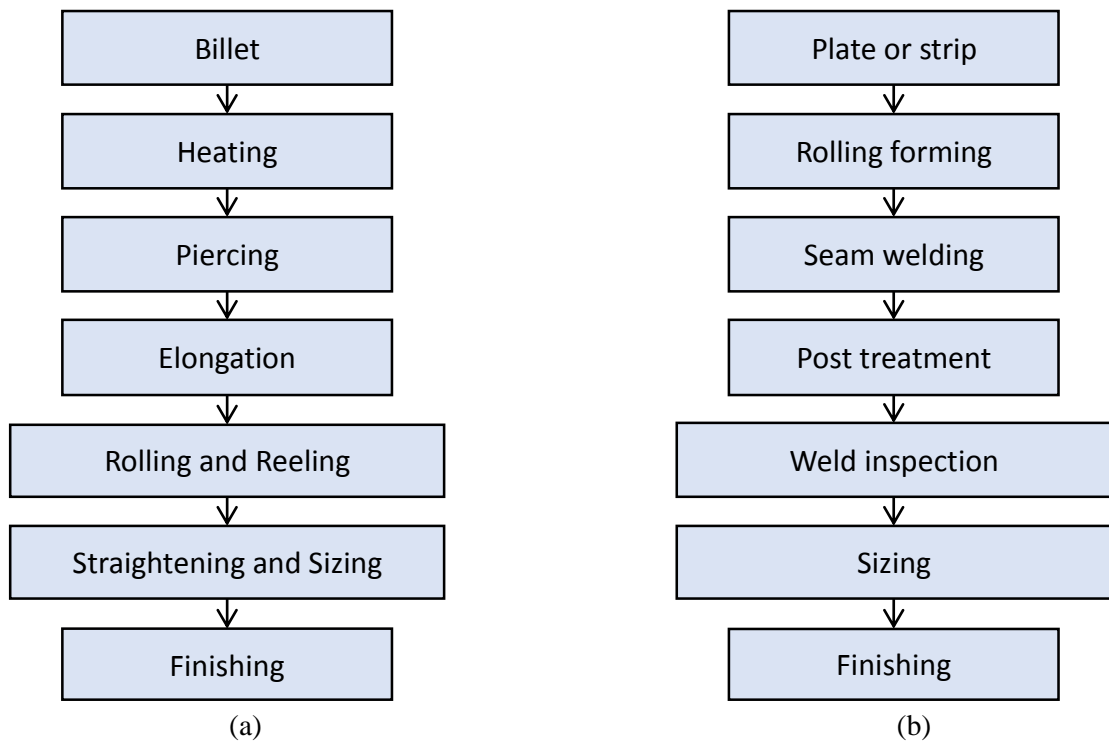


Figure 2.2: Manufacturing process (a) Seamless (b) Seam [14]

2.4 Material Properties of Exhaust Pipe

Exposed to high operating temperature, hot end of the exhaust system is needed to be built with materials of high-temperature strength, thermal fatigue properties, oxidation resistance and salt corrosion. Table 2.1 shows operating temperatures required for exhaust component used in the real application with functions of each component and their service temperature. Selection of material at the cold end should not neglect and vitally needed in order to permit while carrying intended function. Specific functions and required properties and most suitable materials used for each of these applications, described in Table 2.2.

Table 2.1: Exhaust Component functionality and service temperature [15]

Components	Functions	Service Temperature Requirements
Exhaust Manifold	Low thermal mass and durability	750-950
Catalytic Converter	Converts toxic gases into non-toxic gases	1000-1200
Exhaust Muffler	Noise attenuation	100-400
Pipes	Interlinking the exhaust system component regulates the flow of gases.	400-600

Table 2.2: Exhaust component's material requirements [16]

Components	Properties Requirements	Materials Requirements
Exhaust Manifold	<ul style="list-style-type: none"> High-temperature strength Thermal fatigue life Oxidation resistance 	SUS 429LM, SUS 441L, SUS 304
Catalytic Converter	<ul style="list-style-type: none"> High-temperature strength High-temperature salt damage resistance 	SUS 439L, SUS 430, SUS 441L
Exhaust Muffler	<ul style="list-style-type: none"> Corrosion resistance at inner surface (condensate) Corrosion resistance at outer surface (salt damage) 	SUH 409L, SUS 439L, SA1D, SUS 436, SUS 430J1L, SUS 436J1L
Pipes	<ul style="list-style-type: none"> Corrosion resistance at inner surface (condensate) Corrosion resistance at outer surface (salt damage) 	SUH 409L, SUS 439L, SA1D, SUS 436, SUS 430J1L, SUS 436J1L

CHAPTER 3: METHODOLOGY

3.1 Project Flow Chart

Figure 3.1 shows the flowchart constructed accordingly in order to complete the research. This flow chart shows the steps were taken throughout the research gathering material until analysis of the component.

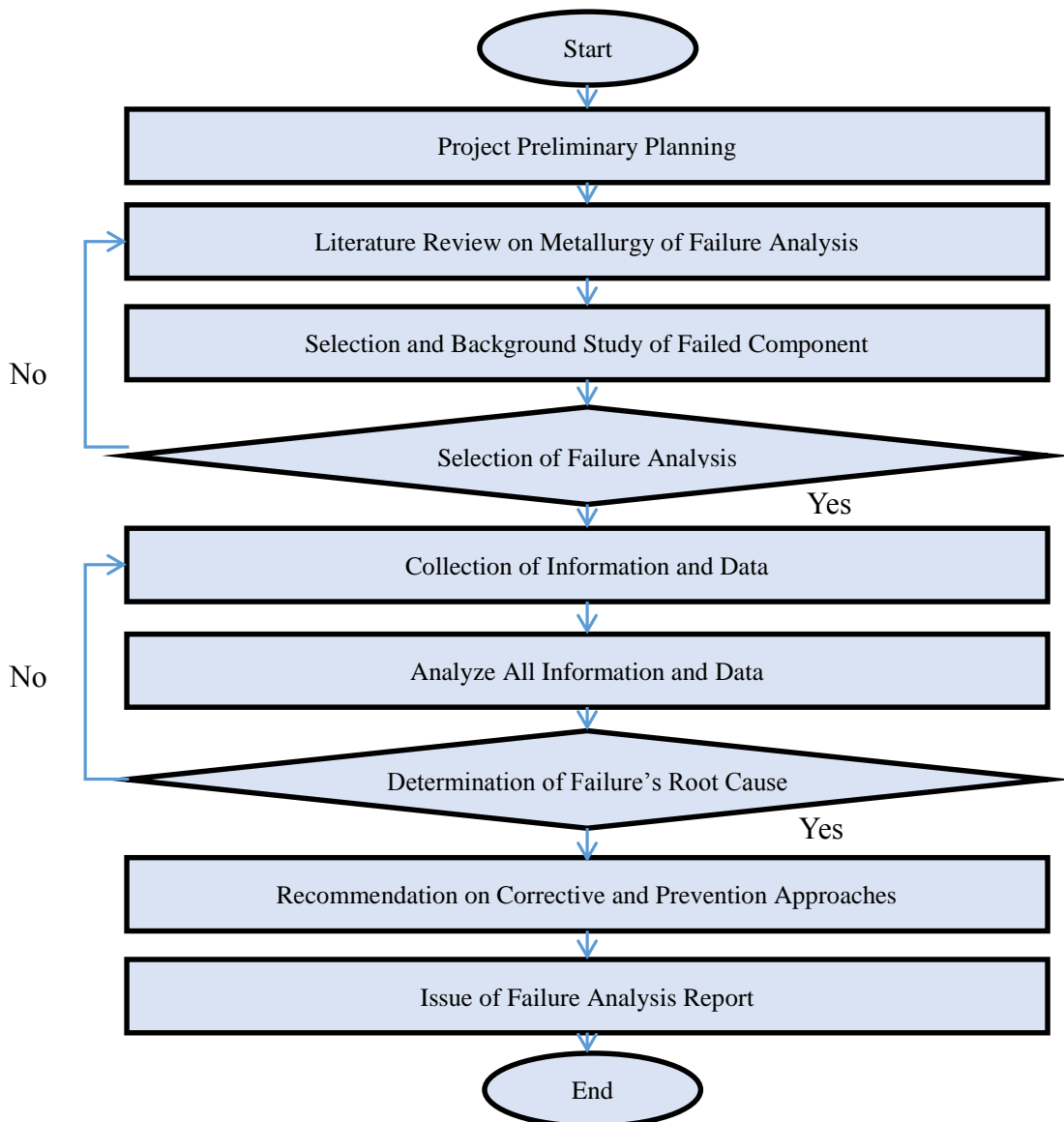


Figure 3.1: Project flow chart

3.2 Project Gantt Charts

Table 3.1 and Table 3.2 show the research Gantt charts. All research activities throughout these two semesters are listed and arranged accordingly in order to be completed within the time frame. Key milestones also have been highlighted in the Gantt chart for each semester.

Table 3.1: Project Gantt chart FYP (1)

Detail of Work	Weeks													
	1	2	3	4	5	6	7	8	9	10	11	12	13	14
1. Selection project topic	Progress													
2. Information gathering		Progress	Progress	Progress										
3. Preparation of extended proposal report			Progress	Progress										
4. Selection of failed component				Key Milestone	Key Milestone									
5. Proposal defense						Key Milestone	Key Milestone							
6. Background study of failed component						Progress	Progress	Progress	Progress	Progress	Progress	Progress	Progress	
7. Preliminary examination of failed component								Progress	Progress					
8. Selection of testing for failed component										Key Milestone	Key Milestone			
9. Macroscopic examination of component												Progress	Progress	
10. Preparation of interim report														Progress

 **Progress**
 **Key Milestone**

Table 3.2: Project Gantt chart FYP (2)

Detail of Work	Weeks													
	1	2	3	4	5	6	7	8	9	10	11	12	13	14
1. Simulation analysis	Key Milestone	Key Milestone	Key Milestone	Key Milestone										
2. Material preparation		Progress	Progress											
3. Material composition analysis			Progress	Progress										
4. Computer Fluid Dynamic simulation analysis				Key Milestone	Key Milestone	Key Milestone	Key Milestone	Key Milestone						
4. Hardness testing						Key Milestone								
5. Microscopic analysis						Progress	Progress							
6. Determination of failure mechanism							Progress	Progress						
7. Analyze data and recommendations								Key Milestone	Key Milestone	Key Milestone				
8. Thesis writing							Progress	Progress	Progress	Progress	Progress	Progress	Progress	Progress
9. Preparation of dissertation and report												Progress	Progress	Progress
10. Submission of dissertation													Key Milestone	Key Milestone
11. Viva														Key Milestone



By constructing Gantt charts it provides a visual timeline for starting and finishing specific duties in completing the research. These charts offers an understandable approach maintaining timescale-based tasks by providing overview of milestones and other key dates thus keep the research progress on track.

3.3 Key Milestones

Figure 3.2 shows the key milestone of this research. There are nine key milestones to be completed in order to accomplish the objective of the research.

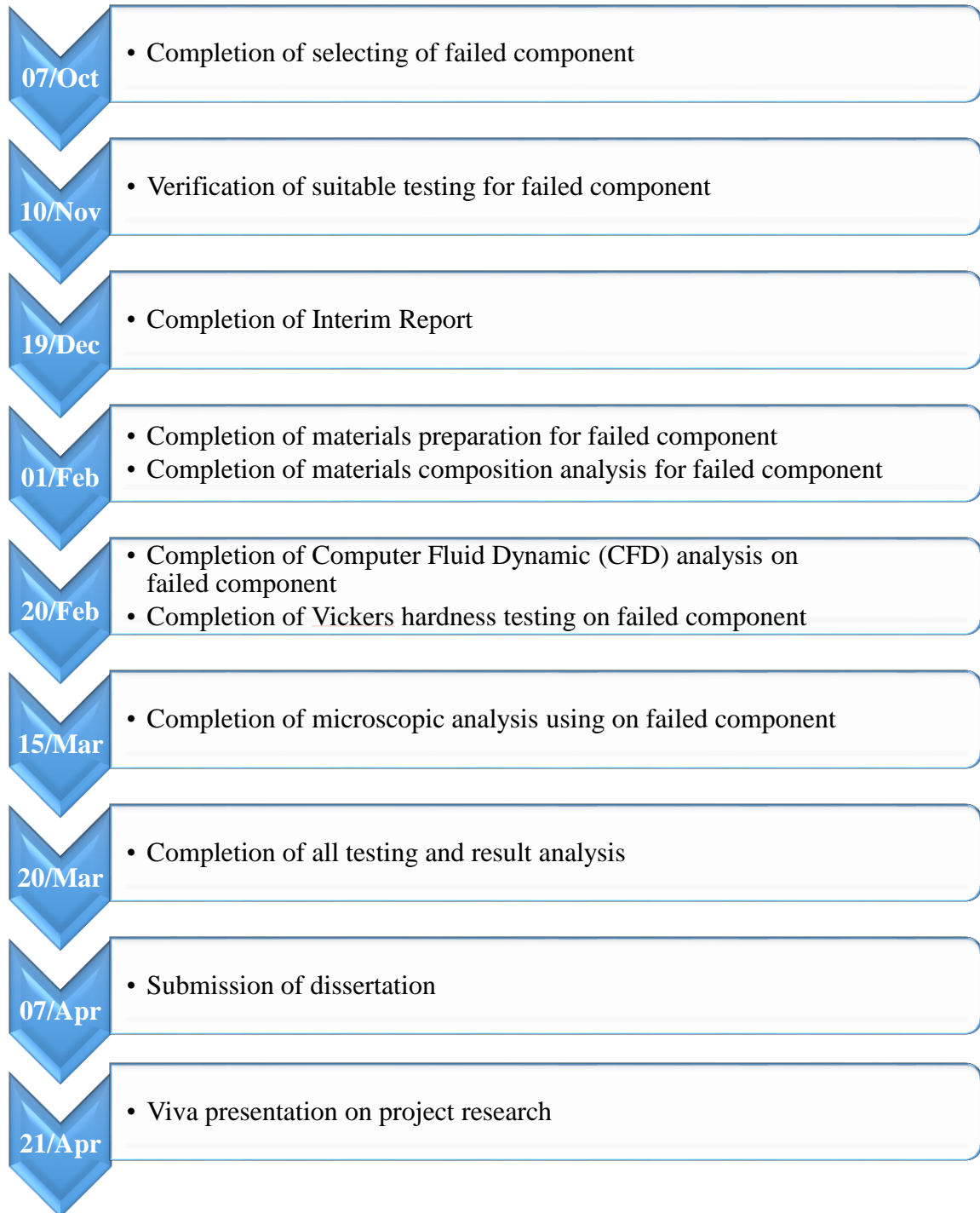


Figure 3.2: Key milestones

3.4 Working Principle Failure Analysis

Failure analysis is an engineering methodology to determine how and why equipment or a component has failed. Although the failed component was produced from metal or plastic or a combination of these materials, the investigation is performed in significant manner. Basically, failure analysis process involves the ability to relate documented chain of information into accurate conclusion on the root cause of the failure. In addition, understandings on the possible condition of failure could prevent the same failure for occurring in the future. The general steps to conduct a comprehensive failure investigation, is as follows [17]:

1. Gathering data for background selected sample
2. Preliminary examination of failed part
3. Analysis using Non-Destructive Test (NDT) and mechanical testing
4. Selection, identification, prevention and/or cleaning of specimens
5. Macroscopic examination and analysis
6. Microscopic examination and analysis
7. Sample preparations analysis of metallographic specimens
8. Determination of failure mechanism
9. Chemical analysis on selected sample
10. Analysis of fracture mechanics
11. Simulation analysis under service condition
12. Analysis of evidence, constructing of conclusion and recommendation

However, many studies and researches on the failure part clearly show that the occurrence of the failure could not be stopped. Facts shown that the failure analysis and laboratory testing conducted provide alternatives to avoid future failures. Alternatives such development on the design, manufacturing process, materials selection, and also the lowering maintenance cost also are provided [18]. In addition, to achieve accurate and reliable analysis, a close study of failure and deep understanding of its operating history are of main significance.

3.4.1 Non-Destructive Testing (NDT) Analysis

Metallographic Analysis

Preliminary examination also known as visual examination was used to analyse failure surface. Typically, the examination is conducted to gain information such as stress concentration, materials imperfection, and presence of coating, case hardened regions, weld and other structure details that contribute towards crack aided by a low-powered magnifier. From the analysis, investigator could identify the mode of failure from the fracture surface i.e. brittle, ductile, fatigue [19] However, the successfulness of this technique depends on the perceptive power of the investigator.

During the preliminary examination process, any relevant depositions in the vicinity of the failure need to be recorded and analysed [20]. Useful data on defectiveness area such an extent of damage, and location of main failure are needed. The information is important to improve and make a better judgement on the failure impression. However, a further investigation under metallographic analysis needs to be carried out in order to clarify the condition of failure surface and clear-out conclusion can be made. Several other NDT analyses are extremely useful depending on types methods of fabrication and type of material. For metal failure investigation, most suitable methods are magnetic particle inspection, etching inspection and liquid penetrant examination [21].

The innovation of Scanning Electron Microscope (SEM) allows a small portion of specimen to be examined at extreme depth focus at a high magnification. High magnifications up to 1,000,000x offered information such as surface topography, crystalline structure, chemical composition and electrical behaviour [22]. In order to achieve, the wavelength of imaging radiation must be reduced. The electrons used in SEM are usually accelerated to high energies of between 2 and 1000 keV (i.e. wavelengths of 0.027-0.0009 nm) [23]. SEM successfully illustrates the failure surface including uniformity and size of grain structure with high depth of focus images that is used to interpret root cause of failure.

Computational Fluid Dynamics (CFD) Analysis

Computational Fluid Dynamics (CFD) Analysis is regarded as one of useful numerical tools for structural analysis to obtain approximate solution of engineering problems. By using this method, the complex body continuum is discretized into simple geometric shapes. A set of linear or nonlinear equations is usually obtained when the loads and boundary conditions are applied. Loads refers to boundary conditions and externally or internally applied forcing functions.

The numerical solution of heat transfer and fluid flow phenomena can begin when the principles governing these processes have been expressed in the mathematical form in terms of differential equations. In the present work, the flow of exhaust gas and heat transfer from the gas is represented by a set of conservation equations of mass, momentum and energy considering the appropriate boundary conditions.

Continuity of Energy Formulas [24]

- Mass

$$\frac{\partial(\rho)}{\partial t} + \frac{\partial(\rho U)}{\partial x} = 0 \quad (1)$$

- Momentum

$$\frac{\partial(\rho U)}{\partial t} + \frac{\partial(p + \rho U^2)}{\partial x} = \frac{\partial}{\partial x} \left(\mu \frac{\partial U}{\partial y} \right) + \frac{\partial}{\partial y} \left(\mu \frac{\partial U}{\partial x} \right) \quad (2)$$

- Energy

$$\frac{\partial(\rho u)}{\partial t} + \frac{\partial(\rho U u + p U)}{\partial x} = \frac{\partial}{\partial x} \left(\frac{k}{c_p} \frac{\partial T}{\partial x} \right) + \frac{\partial}{\partial y} \left(\frac{k}{c_p} \frac{\partial T}{\partial y} \right) \quad (3)$$

Where,

U = Velocity

ρ = Density

P = Pressure

T = Time

x and *y* = distance

3.4.2 Destructive Testing (NDT) Analysis

Vickers Hardness Testing

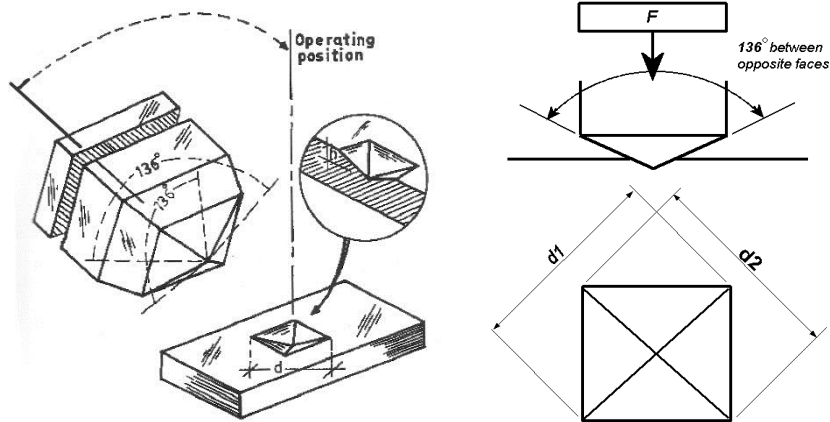


Figure 3.3: Vickers hardness testing mechanism [25]

For Vickers hardness testing as shown in Figure 3.3, a load was applied smoothly on the surface of the sample by forcing the diamond indenter into the samples and held for 15 seconds. In order to get precise results, the physical of the indenter and the accuracy of the applied load need to be controlled. The two impression diagonals are measured after the load is detached. The Vickers Hardness (HV) value could be obtained using the following formula:

$$HV = \frac{1.8544 P}{d^2} \text{ kgf/mm}^2 \quad [26] \quad (4)$$

where P is expressed in kgf and d in mm. Since the units of gram-force (gf) and micrometers (μm) are normally used in this field, the constant of the equation modified to accommodate the conversion factors to ease use during computation. The equation for HV, is expressed in kgf/mm^2 , as follows:

$$HV = \frac{1854.4 P'}{d'^2} \text{ kgf/mm}^2 \quad [26] \quad (5)$$

CHAPTER 4: RESULTS AND DISCUSSION

4.1 Review of the Background Information

Once the incident location area is discovered, it was recognized that the fractured piping was connected to exhaust muffler with the flange to form a major foundation for the main exhaust pipe. The exhaust pipe made up from carbon steel with 35° bend at the middle has length of 230mm pipe. From the observation, a blend of shiny and uneven profile can be seen on the surface texture of main failure region. Main assumption had been made where flow profile in the exhaust pipe leads to a severe pipe thickness loss. Potential enlightenments due to possible root causes of the exhaust pipe failures are listed as follows:

- i. Bad operating condition
- ii. Exhaust pipe mechanical defect.
- iii. Exhaust pipe material defect.

Further observation discovered a large portion of the exhaust pipe affected and damaged by corrosion. The inner surface of the exhaust pipe was strongly affected by the corrosion problem. Some sediments and corrosion products removed from entire inner surface of the pipes indicates that corrosion is occurred uniformly along the pipe. Several pits formation with different sizes and depths were observed in few areas leads directed to serious corrosion problem which leads to leakage occurred from the inside out of the pipe. In addition, some failures of the system's components, mainly at pipe elbows, appeared to be directly correlated to impingement due to extreme fluid flow during service life. Fault tree Analysis (FTA), shown in Figure 4.1 was used as one of Root Cause Analysis (RCA) tools to pinpoint possible failures in the exhaust pipe.

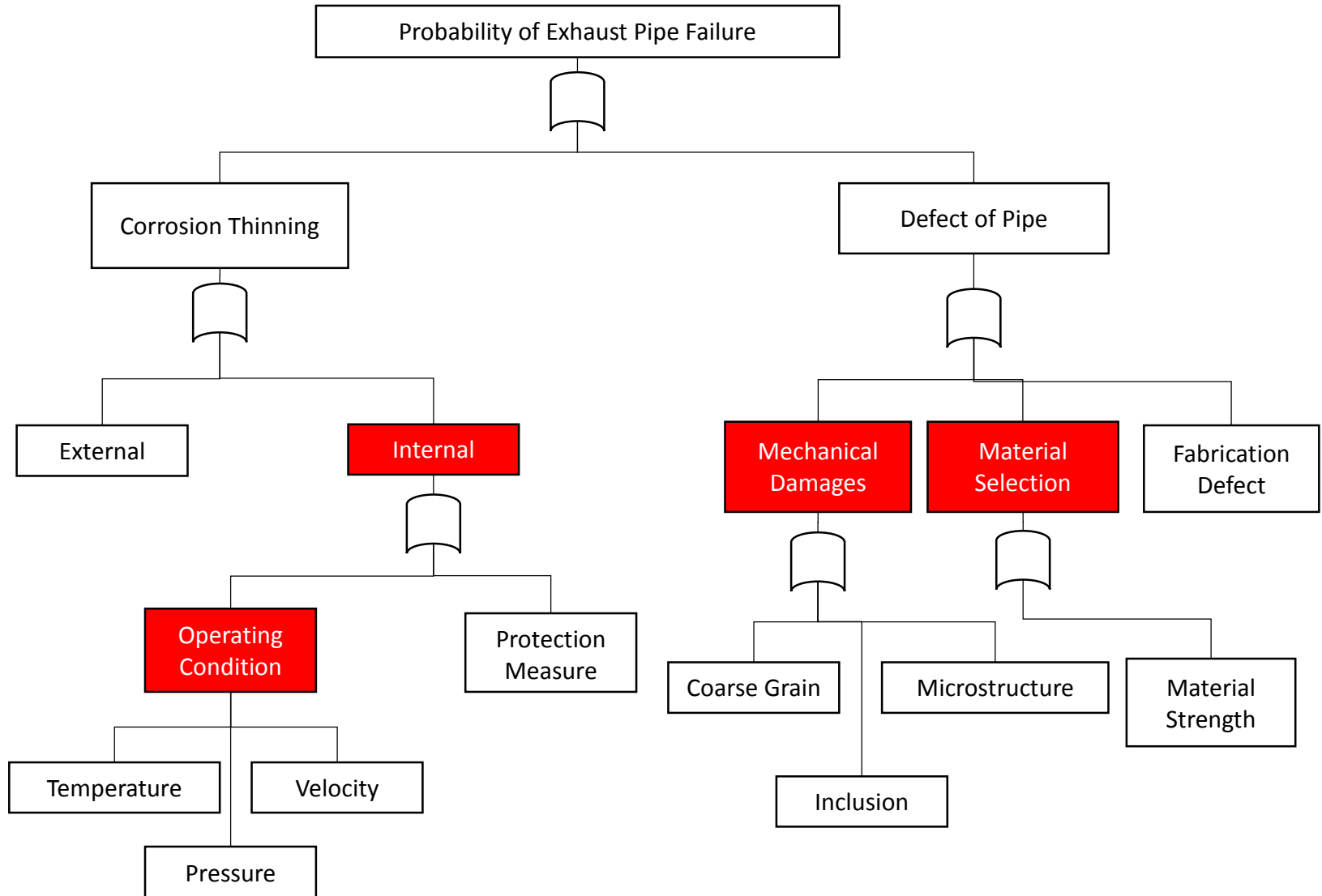


Figure 4.1: Fault tree analysis (FTA)



Figure 4.2: Condition of exhaust pipe studied

Figure 4.2 show the impairment incidents at the elbow of exhaust pipe. The exhaust system was disassembled after the failure occurred. Visual inspections were completed and it was observed that there are a number of leakages along the exhaust pipe especially at the elbow of the pipe. The largest hole was found at the bottom of the elbow exhaust pipe. Wall thinning phenomena can be found in the same area around midline direction of the exhaust pipe. Preliminary data of the exhaust pipe are tabulated in the Table 4.1.

Table 4.1: Preliminary data of the exhaust pipe

Parameter	Details
Type of pipe	Seamless
Internal diameter (mm)	43.00
External diameter (mm)	51.00
Wall thickness (mm)	8.00

4.2 Material Properties of Exhaust Pipe Analysis

4.2.1 Composition Examination

Sample was cut by cross sectional from near the leak end at the elbow of the exhaust pipe and prepared for metallurgical examination. As listed in Table 4.2, the measured composition of the exhaust pipe material is consistent with high carbon steel [27] as referred Appendix B using of Energy Dispersive X-ray (EDX) spectroscopy.

Table 4.2: Chemical composition of the samples

Chemical Composition of the Samples (wt. %)						
Fe	C	Cu	Cr	Mn	Si	P
86.2	13.1	0.3	0.2	0.1	0.1	0.1

4.2.2 Vickers Hardness Test

Before undergoing Vickers hardness tests, samples for were grinded and polished using conventional metallographic methods. The hardness of three samples was measured at different locations using the LEKO Microhardness Tester as referred to Appendix A with a high load of 50kgf, 100kgf, 200kgf and 300kgf according to ASTM E92. The condition for testing was set up as tabulated in Table 4.3. The Vickers indentation was examined under an optical microscope and the diagonals of the indentation measured in order to obtain Vickers hardness values. The hardness values for all samples were compared.

Table 4.3: Vickers test (1) conditions

Number of sample (s)	Four
Applied force, kgf	50, 100, 200, 300
Dwell Time, s	15
Indenter type	Vickers Diamond

Vickers diamond utilized to test the sample hardness at various locations as shown in Figure 4.3. The imprints of symmetric square shape after the Vickers indentation tests were measured using an optical microscope and the Vickers hardness values were calculated and tabulated.

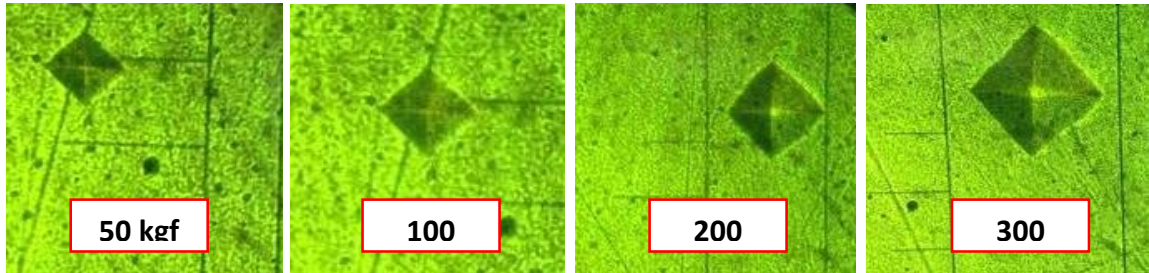


Figure 4.3: Different size of imprint diameters

Figure 4.3 shows indentation with different diameter for Vickers indentation test for different load applied on the surface of the samples. Formula constructed below illustrates that Vickers indentation obeys Meyer law. The correlation between the applied load P and indentation diameter d is as follows:

$$P = kd^m \quad (6)$$

Where m is Meyer index and k is a material constant.

The hardness value calculated using Meyer Law equation as in Equation 3.5 and graph of the applied load against the Vickers Hardness (HV) is shown in Figure 4.4. Throughout the test, rough surface finish of the sample that makes two diagonals of the indentation is difficult to be measure, leading to some significant inconsistency in the hardness calculation. Therefore, the hardness test was repeated in order to obtain an average Vickers Hardness (HV) value thus reduces random errors.

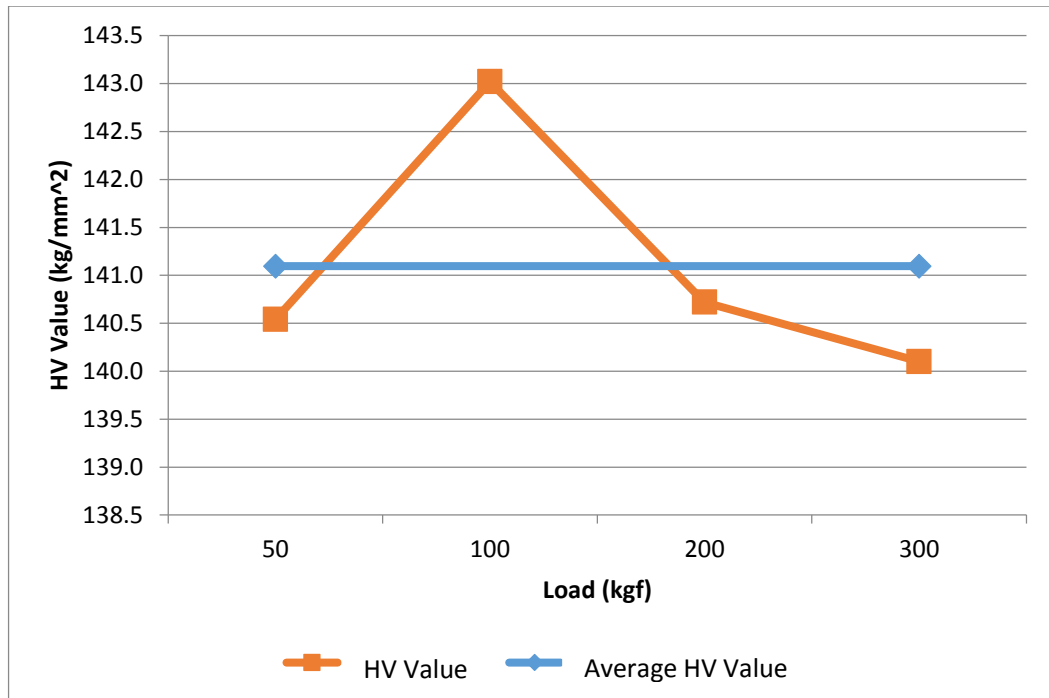


Figure 4.4: Load vs HV values graph

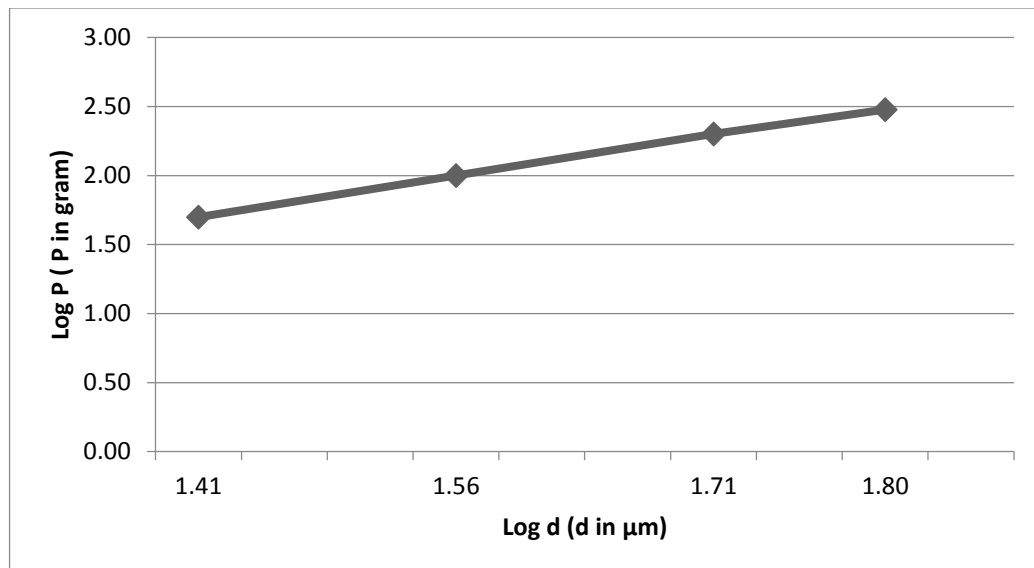


Figure 4.5: Log d vs Log P graph

In the study, it was found out the value of m was 2 and the average of Vickers hardness value was 141.1. According to Onitsch, the value of m for hard materials range from 1 to 1.6, and for soft materials it is more than 1.6. Therefore, it can be concluded that the samples tested in this research can be classified as soft materials [29].

By using an optical microscope, the imprints of the indenters after the Vickers indentation tests were measured and the Vickers Hardness (HV) value were calculated. The hardness calculated Vickers test for all samples are recorded. The test conditions are summarized in Table 4.4.

Table 4.4: Vickers test (2) conditions

Number of sample(s)	One
Applied force, kgf	100
Dwell Time, s	15
Indenter type	Vickers Diamond

Applied force of 100kgf was selected considering 8mm thickness of the specimen and to reduce the error during determination of imprint diameter. Figure 4.6 shows the Vickers Hardness (HV) values calculated based on imprint diameter formed on the specimen using Equation 3.5.

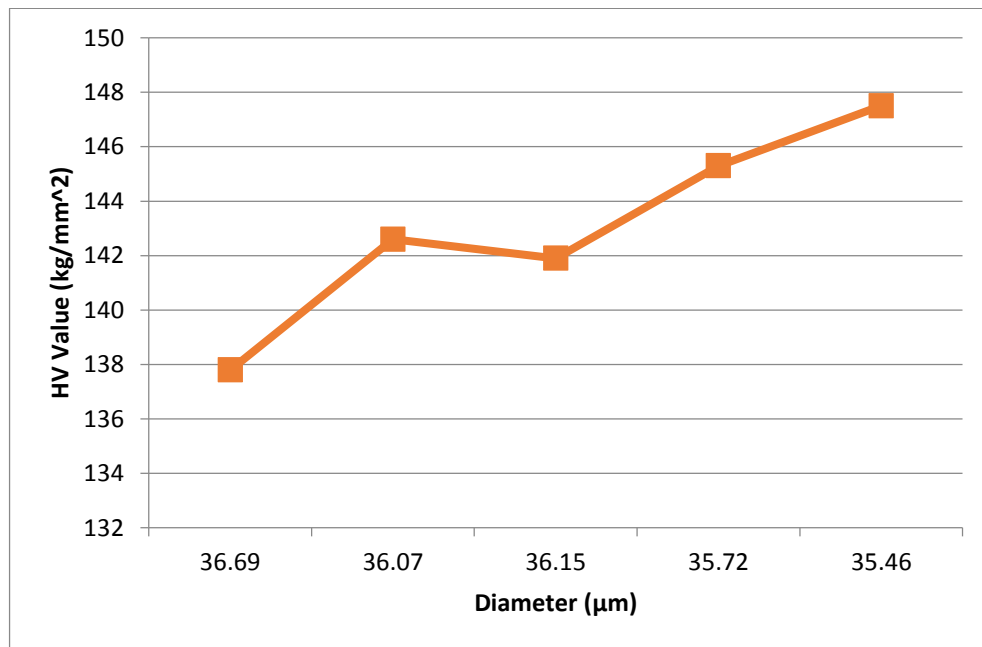


Figure 4.6: Diameter vs HV Values graph

From the result obtained, it was found out that the Vickers hardness values increased as the diameter of imprints increased. In the study, we found that the average diameter of indenter imprints was 36.02 μ m. However data recorded shown inconsistency in Vickers hardness values due to systematic error and random errors. Systematic error donated by various position of eye during determination of imprints diameters. During Vickers hardness testing individual tend to measure an indent diameter is slightly undersized or oversized. Besides, low quality of polish, poor surface finish, and low reflectivity reduce the feasibility of conducting Vickers hardness test producing rough surface finish contribute to random error.

The Vickers hardness testing was conducted several times at different locations and the average value of Vickers Hardness was calculated in order to reduce random error. Table 4.5 shows the Vickers Hardness (HV) values calculated based on imprint diameter and force applied on the specimens.

Table 4.5: Vickers hardness values

	Test 1	Test 2	Test 3	Test 4	Test 5	Average
Vickers Hardness (HV) Value	137.8	142.6	141.9	145.3	147.5	143.0

An equivalent tensile strength was estimated approximately using Vickers Hardness (HV) value obtained previous experiment referred Appendix C [32]. Based on data, the exhaust pipe meets the required tensile strength for material currently used for exhaust pipe application as referred Appendix D [31] shown in Table 4.6. Therefore, it provides strong evidence to conclude that the exhaust pipe has no material defects.

Table 4.6: Requirement of material strength [31]

	Yield Strength (N/mm²)	Tensile Strength (N/mm²)	Elongation (%)	Hardness (HV)
SUH 409L	175 Min	360 Min	25 Min	175 Max
SUS 439L	175 Min	360 Min	22 Min	200 Max
SUS 436	245 Min	410 Min	22 Min	200 Max
SUS 430J1L	205 Min	390 Min	22 Min	200 Max

4.3 Analysis on Failure Area of Exhaust Pipe

A Preliminary examination was conducted on the section of impaired part of exhaust pipe discovered incident of leakage of pipe which led to initial conclusion that the failure was directly caused by the influence of flow stream of the pipe. Therefore, a physical and metallurgical analysis was follow, were conducted on the pipe.

- a) Photo-documentation of visual examination of exhaust pipe.
- b) Metallographic analysis of the damaged exhaust pipe using an optical microscopy and Scanning Electron Microscope (SEM).

4.3.1 Visual Examination

The exhaust pipe was fully examined as full physical component and all photos were analyzed. Based on the preliminary examination on the exhaust pipe, the following observations were made:

- a) The exhaust pipe has the largest hole at the elbow of the pipe situated at the outer of the pipe measuring 23mm x 48mm (length x width).
- b) Internal corrosion indicated as scale and deposit were found on the inner surface of the exhaust pipe.
- c) A significant wall thickness thinning was observed at the failed area with hyperbolic shaped hole at the elbow of the pipe as illustrated in Figure 4.7.

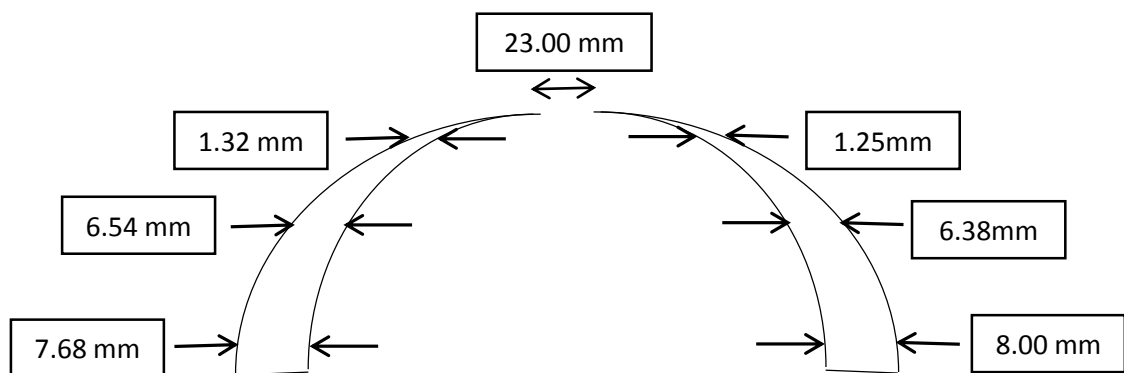


Figure 4.7: Schematic diagram thickness reduction of exhaust pipe

4.3.2 Metallographic Analysis

Microstructural analysis on the exhaust gas was carried out to determine the occurrence of microstructural deficiencies at the failure area. Consistency of microstructural behaviour at the failure region may lead to crucial and strong conclusion on the root cause of the pipe failure by comparing with another section away from the failed region which assumed to be the unaffected area.

The examination was conducted on two specimens at location away from the leak hole while another specimen was taken at the failed region. The specimen were polished and etched using Nital solution (100 ml Ethanol and 10ml Nitric Acid) [32]. The prepared specimens were examined with various high magnifications using an optical metallographic microscope and Scanning Electron Microscope (SEM) as referred Appendix A.

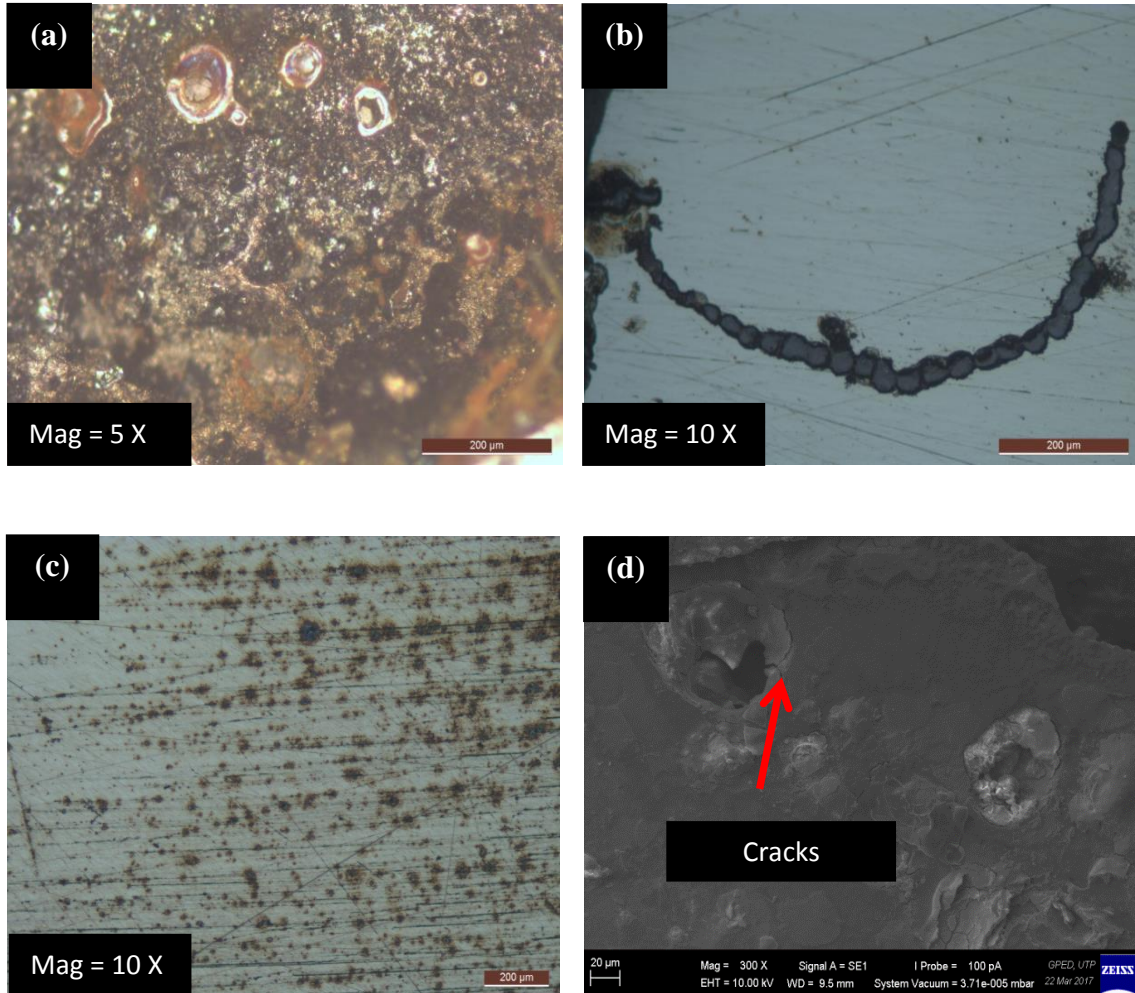


Figure 4.8: (a) Surface morphology of exhaust pipe (b) Linking of pits (c) Various size of pits formation (d) Crack propagation between pits

Figure 4.8(c) indicates various irregular shaped pits of unequal sizes randomly scattered. Frequently observed occurrence of cracks forming caused by sustained load or cyclic load shown by linking of pits in Figure 4.8(b). Formation of cracks is vaguely observed as link pitting formulated which lead to several site impairments. Localized corrosion process shown in Figure 4.8(a) causes propagation of microscopic holes linking to one another on steel surface. The initiation of pitting corrosion is due to the presence of local defects at the metal surface such as flaws in the oxide or segregates of alloy elements, and the presence of aggressive chlorides in the environment [33]. Crack propagation between the pits could be seen in Figure 4.8(d) under a high magnification. This initiates an opening thus leads to surface perforation.

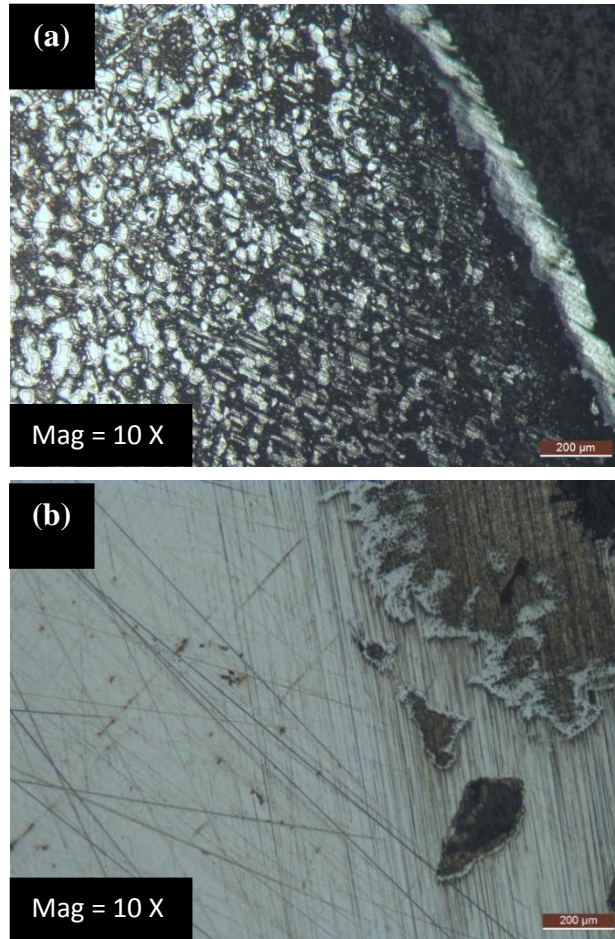


Figure 4.9: (a) Surface oxidation (b) Decarbunisation

Figure 4.9(a) shows surface oxidation or also known as scaling. Phenomenon known as high temperature oxidation observed due to effect of hydrogen on aluminium alloys [34]. Formation of oxide rich scale causes the material lost which reduce the thickness of pipe wall and the strength of the exhaust pipe. Some cracks existed across the scale and voids were present along the scale interface. High temperature oxidation caused by elevated-temperature atmosphere affects the surface layer of the exhaust pipe. Moisture contamination in the atmosphere stimulates surface oxidation and sometimes aggravated by Sulphur [35]. Decarbunisation of the exhaust pipe shown in Figure 4.9(b), caused the excavation of the material at the surface and a resulting porosity. Decarbunisation initiates with graphite subtraction on the surface due to the carbon-oxygen reactions producing carbon monoxide or dioxide resulting in poor wear resistance and low fatigue life.

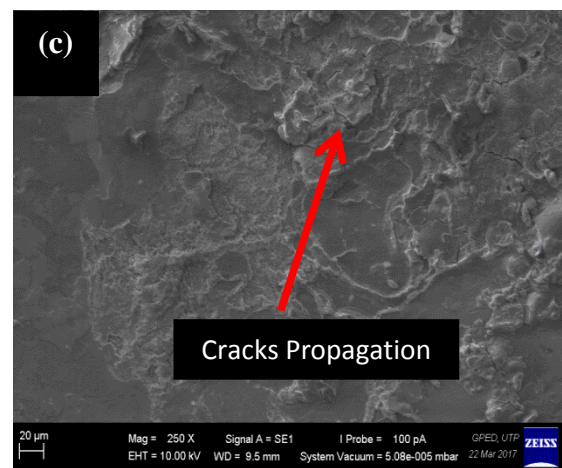
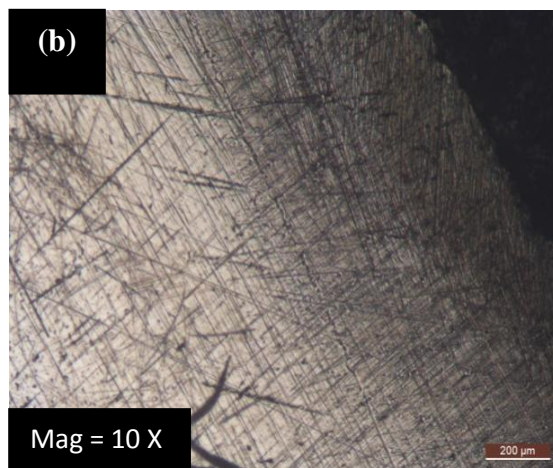
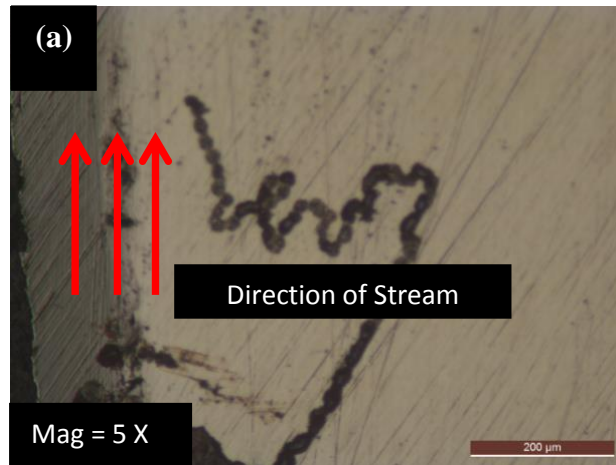


Figure 4.10: (a) Direction of gas stream flow (b) Erosion-corrosion traces (c) Surface cracks

Morphology of erosion site formed at high velocity area for the exhaust pipe steel is shown in Figure 4.10(a). The crack propagation formed suspected creates lumps at the surface of exhaust pipe thus lead to perforation. Figure 4.10(b) and Figure 4.10(c) were taken at the edges of leakage of exhaust pipe and sharp polishing area became relatively blunt and flat. Relative high velocity of fluid flow in the exhaust pipe leaving distinct erosion-corrosion traces. Rough surface features with directional pattern on the metal surface shows the direction of flowing fluid. From the Figure 4.10(b), observed the severe eroded or partly eroded lumps as well as the formation linking of pits. Occurrence of corrosion on the surface become worse due to high fluid velocity and high pressure as surface cracks formed as illustrated Figure 4.10(c).

4.4 Analysis of Exhaust Pipe Flow Field Simulation

This research aimed to study the effect of flow field of the exhaust gas flows through the pipe. ANSYS based numerical analysis is developed for simulation and various curves for flow field within the exhaust pipe. The key operational parameters that are concerned in determining the root cause of failure on the exhaust system are:

- Temperature variation contour over the exhaust pipe
- Pressure variation contour over the exhaust pipe
- Velocity variation contour over the exhaust pipe

The test engine specifications [36] are shown in the Table 4.7.

Table 4.7: Engine specification

Specification	Data
Engine type	CamPro IAFM, 4 Cylinder, DOHC 16V
Displacement	1597 cm ³
Bore x Stroke	76 mm x 88 mm
Compression ratio	10:1
Maximum power	81 KW at 6500 rpm 111 HP at 6500 rpm 109 BHP at 6500 rpm
Maximum torque	148 Nm at 4,000 rpm

The actual dimension of exhaust pipe was taken and material properties of the sample exhaust system are specified in the simulation. For Computational Fluid Dynamics (CFD) analysis, a model of exhaust pipe was drawn through a 3D CATIA program. Table 4.8 shows the key parameter measured from the actual failed exhaust pipe to be used in the Computational Fluid Dynamics (CFD) analysis.

Table 4.8: Exhaust pipe parameters

Parameter	Data
Exhaust Pipe Inner Diameter (mm)	51.00
Exhaust Pipe Outer Diameter (mm)	43.00
Exhaust Pipe Thickness (mm)	8.00
Exhaust Pipe Length (mm)	230.00

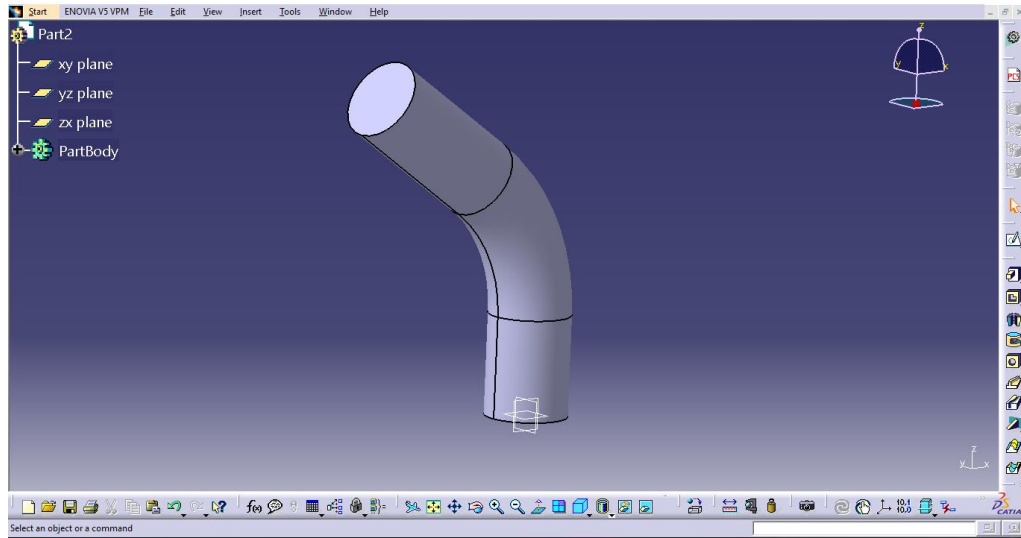


Figure 4.11: Exhaust pipe model

Due to complexity of the design of the exhaust system, some simplifications were done in order to build a reasonable Finite Element Method (FEM) model. This model concentrates on the correlation of flow field to the failure of exhaust pipe as shown in Figure 4.11. This model was important for ANSYS program and it was been meshed using ANSYS Workbench (FLUENT) software. The elements used for meshing are tetrahedral shaped with other default settings in the ANSYS fluent. Details of the mesh are summarized in Table 4.9.

Table 4.9: Mesh result and properties of exhaust model

Parameter	Details
Number of Nodes	26997
Number of Elements	138554
Mesh Quality	0.3
Refinement	2

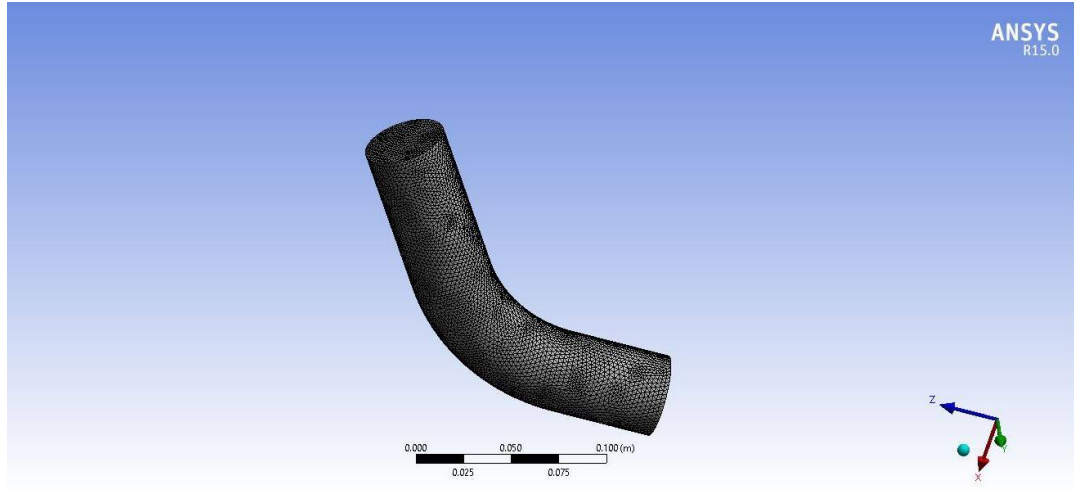


Figure 4.12: Meshed exhaust pipe model

After the meshing process shown in Figure 4.12 the flow analysis was done using fluent by setting various boundary conditions. The inside flow was assumed to be turbulence, so k- ϵ turbulence model used in this study. The air is used as the fluid material in the analysis of muffler. The density was expected to change with temperature so energy equation keeps 'ON' at the time of analysis. At the inlet boundary condition Velocity and Temperature were defined and at the outlet temperature and pressure were defined as boundary conditions. Table 4.10 below shows the test conditions selected as the boundary conditions for Computational Fluid Dynamics (CFD) Analysis.

Table 4.10: Operating conditions of gas stream flow

Parameter	Data
Exhaust gas mass flow rate (kg/s)	0.0115 [37]
Exhaust gas inlet temperature (K)	700 [38]
Exhaust gas inlet pressure (Pa)	300000 [38]
Exhaust gas outlet pressure (Pa)	300000
Heat Transfer Coefficient (w/m^2s)	15

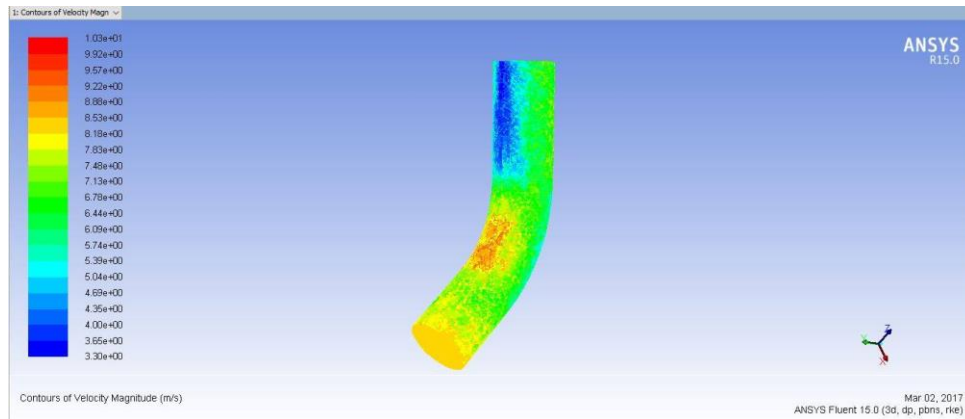


Figure 4.13: Velocity contour

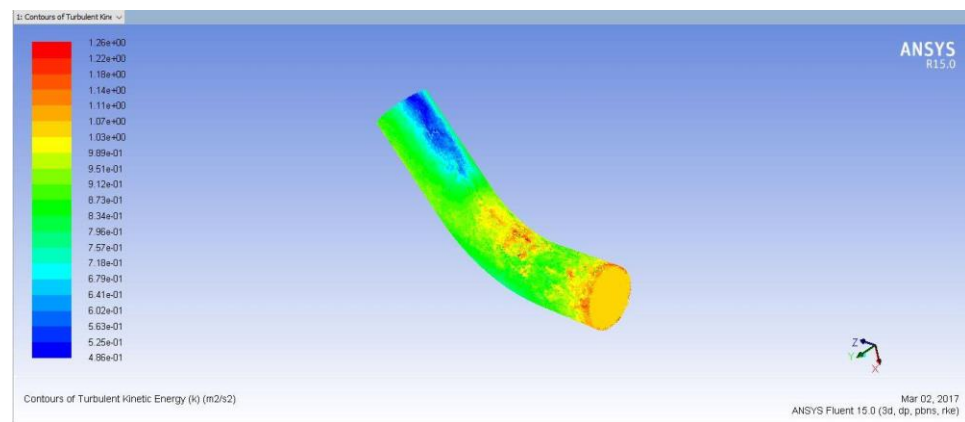


Figure 4.14: Turbulence contour

Velocity values obtained vary between 3.30 m/s and 10.26 m/s as observed in the exhaust pipe. The velocity reduced as expected after passing over the elbow region. The velocity which is about 7.48 m/s at inlet becomes 3.30 m/s in some regions especially at elbow towards the outlet of the pipe. As shown in the Figure 4.14, the high-speed airflow zone of bend exhaust pipe area is mainly concentrated in the middle of inner pipe before the pipe elbow. At the same time, the inner velocity and outer velocity are greatly different one another at the elbow pipe region as illustrated by Figure 4.13.

High fluid flow introduced in Figure by exhaust system leads to erosion-corrosion damage. Perforations of exhaust pipe caused by erosion-corrosion failures allow exhaust leaks in internal components. Besides, solid particles in exhaust gas can rigorously cause erosion damage thus lead to the reduction of wall thickness of exhaust pipe. Corrosion failures may not affect the entire thickness of the pipe but reduces the thickness through pitting corrosion which allows premature fatigue or even a tensile failure.

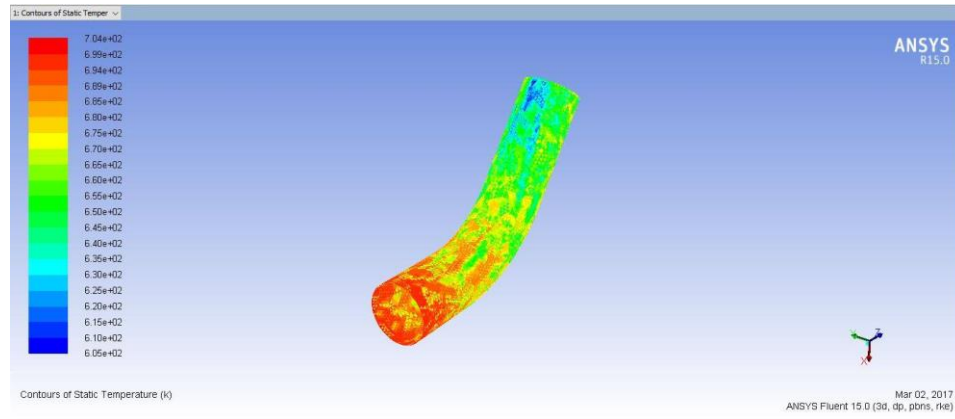


Figure 4.15: Temperature contour

Heat transfer between exhaust gas and pipe wall playing important role in determining the root cause of exhaust pipe failure. Throughout the research, the temperatures were recorded at inlet and outlet of the exhaust pipe. The temperature values of the pipe wall vary between 604K and 704K. It is observed that the temperature in the eroded pipe wall is higher than that in the surrounding areas. High loads in the pipe are expected as a result of rapidly fluctuating exhaust gas pressures, and turbulent hot fluid flow at a high flow rate as illustrated in Figure 4.15.

Exposed to high temperature distribution lead to thermal fatigue cracking consists of oxidation penetrating the pipe surface and creates crack opening. During sustained periods at high temperature, creeps deformation is one of degradation mechanisms in steels accelerated, where tensile stresses experienced is prone to fracture. Tensile failure which is also known as ductile failure occurred as the material failed to sustain the stress imposed. Cyclic exposure at high temperature cause acceleration in diffusion mechanisms that modified the original microstructure of the material prone to decarburization and carburization of pipe surface thus affect the wall thickness of pipe.

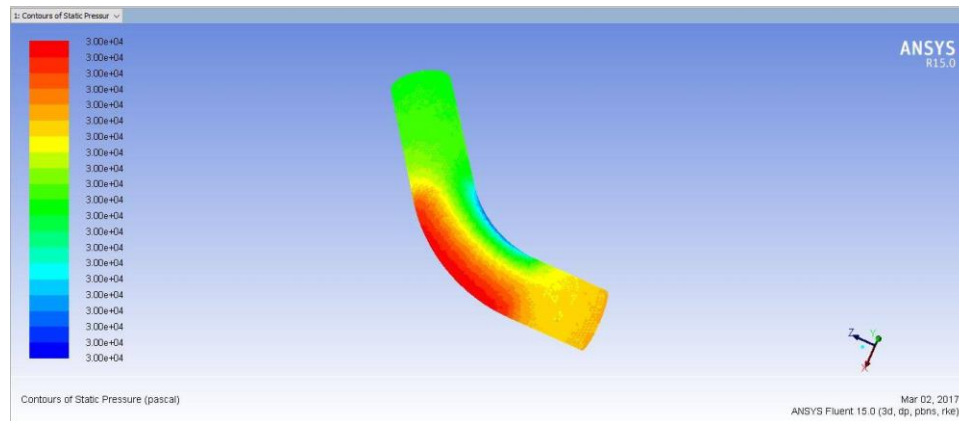


Figure 4.16: Pressure contour

Figure 4.16 demonstrates the pressure gradient in the radial direction is large, showing a small pressure value near the region of the inner wall surface of the pipe with larger distribution high pressure at the outer wall surface area. This is due to the bend curvature of the fluid as the gas exhaust flow contributes centrifugal effect to the radius of curvature larger near the outer wall of the pipe thus leads to plurality of fluid due to push the outer wall surface. In addition, the outer bend exhaust pipe experienced high pressure compare to inner exhaust pipe due to viscous fluid along the pipe wall along the secondary flow and losses arising out of the loss.

Exhaust pipe experience mainly longitudinal cracking and shearing especially during changing direction of flow at the elbow due to high pressure flow of gas exhaust and moments of inertia. Striations on fracture surface indicate the problem related fatigue failure. Material degradation due to corrosion worsened due to high impact of the gas flow inside the exhaust pipe. High stress concentration at the elbow of the pipe is a crucial aspect is designing an installation of the system. Fatigue failure stimulates crack initiation which worsened by high pressure gas flow that responsible for crack propagation somewhere region with high stress values. Stress concentration generated at the pipe wall result into jamming and erosion which ultimately cause perforation of the pipe.

CHAPTER 5: CONCLUSION

5.1 Conclusion

Based to the collected evidence from simulation and testing as well as extensive previous data, the research concludes that the root cause of the failure of the exhaust pipe failures is due to corrosion–erosion. Vickers hardness test regarded one of Destructive technique (DT) indicated the exhaust pipe comply the specification of required tensile strength thus conclude the failure of the pipe cannot be classified as to material deficiency.

Non-Destructive technique (NDT) including metallographic analysis found the failure was originated by crack formation, based on investigation of material properties and behavior of the exhaust pipe. The facts erosion- corrosion mechanism occurred in exhaust pipe was revealed as the inner flow field was simulated using the mixture model based on the correlation flow of exhaust gas.

The Computational Flow Dynamics (CFD) results showed that the affected gradient exists near the elbow of the exhaust pipe at the outer pipe. These gradients exist at regions of high flow velocity, high wall pressure, and high in flow turbulence. These conditions cause crack to enlarge and break off into huge lumps, resulting in the perforations.

Results obtained from Computational Flow Dynamics (CFD) simulations and metallography analysis on the failed area of the exhaust pipe validated as erosion-corrosion mechanism which caused excessive thinning of steel pipe wall thus lead to perforation of the exhaust pipe. Further recommendations and prevention strategies to overcome root cause of failure analyze using Root Cause Analysis (RCA) methods discussed for product development.

5.2 Recommendations

The following approaches are recommended to avoid recurrences of the same failure and to support the exhaust pipe product development of exhaust pipe system in the future.

- Further study on material selection of construction of piping handling the current gas streams condition.
- Minimizing erosion-corrosion by improving the gas stream flow in the pipe.
- Improving the product design by allowing a larger pipe bend angles.
- Using corrosion inhibitors or cathodic protection to minimize erosion-corrosion.

REFERENCES

- [1] Cat-Back Performance Exhaust System Review. (n.d.). Retrieved February 10, 2017, from <https://www.etrailer.com/faq-magnaflow-exhaust-systems.aspx>
- [2] Nelson WB. Accelerated Testing: Statistical Models, Test Plans, And Data Analysis. Hoboken, New Jersey: John Wiley & Sons, Inc; 2004.
- [3] Makhlouf, Abdel Salam Hamdy Aliofkhaezai, Mahmood. (2016). Handbook of Materials Failure Analysis with Case Studies from the Aerospace and Automotive Industries - 18. Failure Mechanisms and Modes Analysis of Vehicle Exhaust Components and Systems. Elsevier. Online version available at: <http://app.knovel.com/hotlink/pdf/id:kt01101EQ2/handbook-materials-failure/failure-mechanisms-modes> Retrieved November 26, 2016.
- [4] Rosenfeld,& Kiefner. (2006). *Basics of Metal Fatigue in Natural Gas Pipeline Systems – A Primer for Gas Pipeline Operators*. Retrieved February 5, 2017, from <http://www.ingaa.org/File.aspx?id=29880&v=b74aa315>
- [5] Simms , H. G. (2011). *Oxidation Behaviour Of Austenitic Stainless Steels At High Temperature In Supercritical Plant*. Retrieved January 24, 2017.
- [6] Jebanski. (n.d.). *Calculation of Tail Pipe Noise of Exhaust System with Wave*. Retrieved February 5, 2017.
- [7] Lochbaum. (2015, November 17). The Bathtub Curve, Nuclear Safety, and Run-to-Failure. Retrieved January 24, 2017, from <http://allthingsnuclear.org/dlochbaum/the-bathtub-curve-nuclear-safety-and-run-to-failure>
- [8] Exhaust System Repairs. (n.d.). Retrieved February 5, 2017, from <http://www.engeautomotive.com/auto-repair/exhaust/index.php>
- [9] Agilesh. & .Pichandi (2016). International Journal for Research in Applied Science & Engineering Technology (IJRASET). *Design and Analysis of Exhaust*

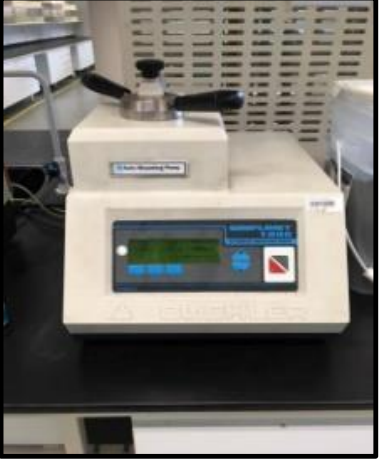

- Manifold in Diesel Engine*. Retrieved April 1, 2017, from <http://www.ijraset.com/files/serve.php?FID=4017>
- [10] Cvetkovski (n.d.). *Influence Of Thermal Loading On Mechanical Properties Of Railway Wheel Steels*. Retrieved April 11, 2017.
- [11] M., S., K., & D. (n.d.). *Thermal And Structural Analysis Of Exhaust Manifold Using Fea Approach*. Retrieved April 9, 2017, from <http://www.ijfeat.org/papers/ME31.pdf?i=1>
- [12] Elements of Metallurgy and Engineering Alloys. (2008). *Fatigue*. Retrieved December 29, 2016.
- [13] Elin M. (2011). *Welded Stainless Steel Tubes & Pipes vs. Seamless*. Retrieved April 10, 2017, from <http://www.outokumpu.com/sitecollectiondocuments/welded-stainless-steel-tubes-and-pipes-vs-seamless-acom.pdf>
- [14] M S J Hashmi (n.d.). *Aspects of Tube And Pipe Manufacturing Processes: Meter To Nanometer Diameter*. Retrieved April 17, 2017.
- [15] Rajadurai, Afnas, Ananth, Surendhar (2014). *Materials for Automotive Exhaust System*. Retrieved April 10, 2017.
- [16] Y. I., & M. K. (2003). Nippon Steel Technical Report. *Present and Future Trends of Stainless Steel for Automotive Exhaust System*. Retrieved April 9, 2017.
- [17] D. Wulpi, Chapter 1: Techniques of Failure Analysis, *Understanding How Components Fail*, 2nd ed., ASM International, 2000, p 1-11.
- [18] I.C.F Canale, R.A Mesquinta, G.E Totten, (Ed.). (2008). *Failure Analysis of Heated Treated Steel Component*. Materials Park, Ohio: ASM International.
- [19] C.R Brooks and A. Choundhury, Chapter 1: Introduction, *Metallurgical Failure Analysis*, McGraw-Hill, 1993, p 1-72.
- [20] R. Graham, Strategies for Failure Analysis, *Adv. Material. Process*, Aug 2004, p 45-50.




- [21] Das, A. K. *Metallurgy of Failure Analysis*. New York: McGraw-Hill, 1997.
- [22] P.M. Mumford, Test Methodology and Data Analysis, Tensile Testing, P. Han, Ed., ASM International, 1992, p 55
- [23] Vernon-Parry, K. D. (2000). Scanning Electron Microscopy: An Introduction, 13(4), 40-44. Retrieved October 6, 2016.
- [24] Sharma. (2011). *Fluid Flow and Heat Transfer Phenomena In An Exhaust Gas Pipe Of An IC Engine*. Retrieved April 19, 2017.
- [25] F. Vander. (1998). Advanced Materials and Processes. *Microindentation Hardness Testing*. Retrieved April 5, 2017.
- [26] W. Gayle. (2012). National Institute of Standards & Technology . *Vickers Microhardness of Steel*, 1-4. Retrieved February 13, 2017.
- [27] D. G. (2005). *Carbon Steel Handbook* . California , USA: Electric Power Research Institute. Retrieved March 10, 2017, from <http://wiki.olisystems.com/wiki/images/0/0c/Carbon-Steel-Handbook.pdf> Retrieved October 9, 2016.
- [28] M. Lakshmipriya. (2012). International Conference on Materials Science and Technology. *Vickers microhardness studies on solution-grown single crystals of potassium boro-succinate*. Retrieved February 15, 2017.
- [29] M. B., O. U., S. A., A. E., & N. U. (2004). Vickers Microhardness Studies of Fe-Mn Binary Alloys. Retrieved April 11, 2017.
- [30] Sunlogic Industrial Solution. (n.d.). *Hardness Conversion Chart*. Retrieved April 10, 2017.
- [31] Daehan Stainless Steel. (n.d.). *Mechanical Property*, 10-11. Retrieved April 10, 2017.
- [32] Zipperian, D. D. (2011). Metallographic Handbook. Retrieved February 9, 2017, from <http://www.metallographic.com/Brochures/Met-Manual-2b.pdf>

- [33] Frankel, G. S. (n.d.). Pitting Corrosion of Metals A Review of the Critical Factors. Retrieved April 9, 2017, from https://kb.osu.edu/dspace/bitstream/handle/1811/45442/FrankelG_JournalElectrochemicalSociety_1998_v145n6_p2186-2198.pdf?sequence=1
- [34] Herring, D. (2016, February 10). High-Temperature Oxidation – A Case Study. Retrieved April 08, 2017, from <http://www.industrialheating.com/articles/92718-high-temperature-oxidation-a-case-study>
- [35] Campbell, F.C.. (2008). Elements of Metallurgy and Engineering Alloys. ASM International. Online version available at: <http://app.knovel.com/hotlink/toc/id:kpEMEA000U/elements-metallurgy-engineering/elements-metallurgy-engineering> Retrieved October 3, 2016
- [36] CamPro engine. (n.d.). Retrieved February 9, 2017, from http://www.wikiwand.com/en/CamPro_engine
- [37] Mesut Durat, Zekeriya Parlak, Murat Kapsiz, Adnan Parlak, & Ferit Fiçici. (2012, June 20). *CFD and Experimental Analysis on Thermal Performance of Exhaust System of A Spark Ignition Engine. (2013)*. Retrieved December 17, 2016.
- [38] Prof. Amar Pandhare, Ayush Lal, Pratik Vanarse, Nikhil Jadhav, & Kaushik Yemul. (2014, May 1). *CFD Analysis of Flow Through Muffler To Select Optimum Muffler Model For CI Engine*. Retrieved December 17, 2016.

APPENDICES

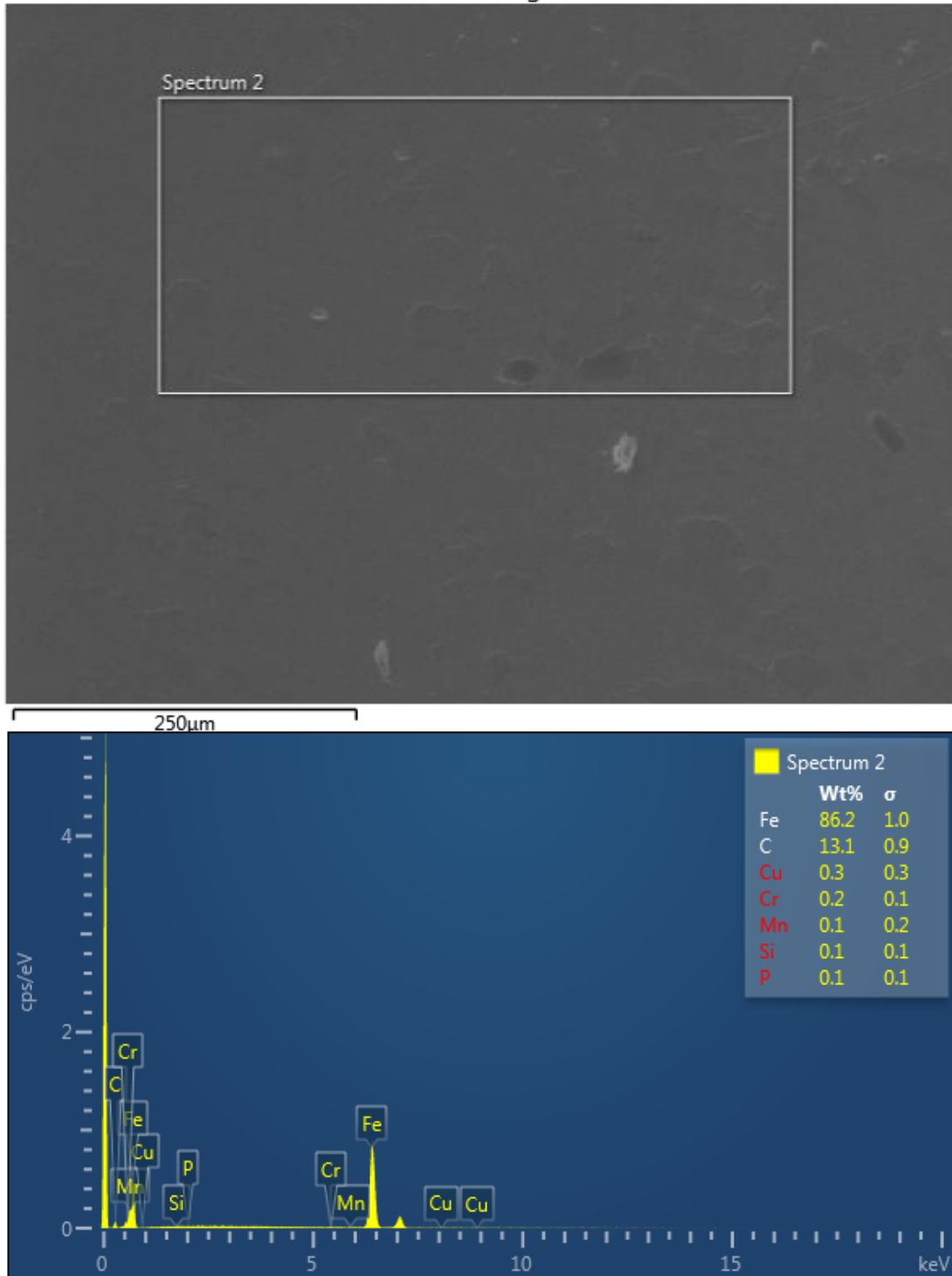
APPENDIX A – TOOLS AND EQUIPMENT

No.	Equipment / Tools	Description
1	Hot Mounting Press Machine	
2	Polishing Machine	

3	Microhardness Tester	 A digital microhardness tester with a white base and a black upper section, featuring a small LCD screen on the front. It is positioned on a dark lab bench in front of a bulletin board with papers.
3	Optical Microscope	 A binocular optical microscope with a white body and black eyepieces, mounted on a black base. It is on a lab bench with a computer monitor and a pink container visible in the background.
3	Scanning Electron Microscope (SEM) And Energy Disperse X-Ray (EDX)	 A large, white scanning electron microscope (SEM) system with a computer workstation (monitor, keyboard, mouse) connected to it, situated on a lab bench.

APPENDIX B – ENERGY DISPERSE X-RAY (EDX) RESULTS

Electron Image 1



APPENDIX C – VICKERS HARDNESS CONVERSION



Hardness Conversion Chart

Brinell Hardness	Vickers Hardness	Rockwell Hardness	Tensile Strength
100 HB	105 HV	- HRC	335 N/mm ²
101 HB	106 HV	- HRC	338 N/mm ²
102 HB	107 HV	- HRC	341 N/mm ²
103 HB	108 HV	- HRC	344 N/mm ²
104 HB	109 HV	- HRC	347 N/mm ²
105 HB	110 HV	- HRC	350 N/mm ²
106 HB	111 HV	- HRC	355 N/mm ²
107 HB	112 HV	- HRC	360 N/mm ²
108 HB	113 HV	- HRC	365 N/mm ²
109 HB	114 HV	- HRC	370 N/mm ²
110 HB	115 HV	- HRC	373 N/mm ²
111 HB	116 HV	- HRC	376 N/mm ²
112 HB	117 HV	- HRC	379 N/mm ²
113 HB	118 HV	- HRC	382 N/mm ²
114 HB	119 HV	- HRC	385 N/mm ²
115 HB	120 HV	- HRC	388 N/mm ²
116 HB	121 HV	- HRC	391 N/mm ²
117 HB	122 HV	- HRC	394 N/mm ²
118 HB	123 HV	- HRC	397 N/mm ²
119 HB	125 HV	- HRC	400 N/mm ²
120 HB	126 HV	- HRC	403 N/mm ²
121 HB	127 HV	- HRC	406 N/mm ²
122 HB	128 HV	- HRC	409 N/mm ²
123 HB	129 HV	- HRC	412 N/mm ²
124 HB	130 HV	- HRC	415 N/mm ²
125 HB	131 HV	- HRC	418 N/mm ²
126 HB	132 HV	- HRC	422 N/mm ²
127 HB	133 HV	- HRC	426 N/mm ²
128 HB	135 HV	- HRC	430 N/mm ²
129 HB	136 HV	- HRC	434 N/mm ²
130 HB	137 HV	- HRC	438 N/mm ²
131 HB	138 HV	- HRC	442 N/mm ²
132 HB	139 HV	- HRC	446 N/mm ²
133 HB	140 HV	- HRC	450 N/mm ²
134 HB	141 HV	- HRC	453 N/mm ²
135 HB	142 HV	- HRC	456 N/mm ²
136 HB	143 HV	- HRC	459 N/mm ²
137 HB	144 HV	- HRC	462 N/mm ²
138 HB	145 HV	- HRC	465 N/mm ²
139 HB	146 HV	- HRC	468 N/mm ²
140 HB	147 HV	- HRC	471 N/mm ²
141 HB	148 HV	- HRC	474 N/mm ²
142 HB	149 HV	- HRC	477 N/mm ²
143 HB	150 HV	- HRC	480 N/mm ²
144 HB	151 HV	- HRC	484 N/mm ²
145 HB	152 HV	- HRC	488 N/mm ²
146 HB	153 HV	- HRC	492 N/mm ²
147 HB	155 HV	- HRC	495 N/mm ²
148 HB	156 HV	- HRC	498 N/mm ²
149 HB	157 HV	- HRC	501 N/mm ²
150 HB	158 HV	- HRC	504 N/mm ²
151 HB	159 HV	- HRC	507 N/mm ²
152 HB	160 HV	- HRC	510 N/mm ²
153 HB	161 HV	- HRC	515 N/mm ²
154 HB	162 HV	- HRC	520 N/mm ²
155 HB	163 HV	- HRC	525 N/mm ²
156 HB	164 HV	- HRC	530 N/mm ²
157 HB	165 HV	- HRC	532 N/mm ²
158 HB	166 HV	- HRC	534 N/mm ²
159 HB	167 HV	- HRC	537 N/mm ²

APPENDIX D – PROPERTIES OF EXHAUST PIPE MATERIAL

MECHANICAL PROPERTY

AUSTENITE

TYPE	KS	YIELD STRENGTH (N/mm ²)	TENSILE STRENGTH (N/mm ²)	ELONGATION (%)	HARDNESS(HV)
301	STS301	205Min	520Min	40Min	218Max
301L	STS301L	215Min	550Min	45Min	218Max
304	STS304	205Min	520Min	40Min	200Max
304L	STS304L	175Min	480Min	40Min	200Max
304JI	STS304JI	155Min	450Min	40Min	200Max
316	STS316	205Min	520Min	40Min	200Max
316L	STS316L	175Min	480Min	40Min	200Max
321	STS321	205Min	520Min	40Min	200Max

FERRITE

TYPE	KS	YIELD STRENGTH (N/mm ²)	TENSILE STRENGTH (N/mm ²)	ELONGATION (%)	HARDNESS(HV)
409L	STR409L	175Min	360Min	25Min	175Max
410L	STS410L	195Min	360Min	22Min	200Max
430	STS430	205Min	450Min	22Min	200Max
430J1L	STS430J1L	205Min	390Min	22Min	200Max
436L	STS436L	245Min	410Min	20Min	230Max
439	STS439	175Min	360Min	22Min	200Max
444	STS444	245Min	410Min	20Min	230Max

MARTENSITE

TYPE	KS	YIELD STRENGTH (N/mm ²)	TENSILE STRENGTH (N/mm ²)	ELONGATION (%)	HARDNESS(HV)
410	STS410	205Min	440Min	20Min	210Max
420J1	STS420J1	225Min	520Min	18Min	234Max
420J2	STS420J2	225Min	540Min	18Min	247Max



DAEHAN SPECIAL STEEL